Distribution Agreement

In presenting this thesis or dissertation as a partial fulfillment of the requirements for an advanced degree from Emory University, I hereby grant to Emory University and its agents the non-exclusive license to archive, make accessible, and display my thesis or dissertation in whole or in part in all forms of media, now or hereafter known, including display on the world wide web. I understand that I may select some access restrictions as part of the online submission of this thesis or dissertation. I retain all ownership rights to the copyright of the thesis or dissertation. I also retain the right to use in future works (such as articles or books) all or part of this thesis or dissertation.

Signature:

_____ _____

Thomas Anderson Date

Calculations of Prebiotic Molecules Formed from $O(^1D)$ Insertion Reactions

By

Thomas Anderson
Master of Science

Chemistry

_____

Susanna L. Widicus Weaver, Ph. D.
Advisor

_____

Michael Heaven, Ph. D.
Committee Member

_____

James T. Kindt, Ph. D.
Committee Member

Accepted:

_____

Lisa A. Tedesco, Ph.D.
Dean of the James T. Laney School of Graduate Studies

_____

Date

Calculations of Prebiotic Molecules Formed from $O(^1D)$ Insertion Reactions

By

Thomas Anderson
B.S. Georgia Southern University

Advisor: Susanna L. Widicus Weaver, Ph. D.

An abstract of
A thesis submitted to the Faculty of the
James T. Laney School of Graduate Studies of Emory University
in partial fulfillment of the requirements for the degree of
Master of Science
in Chemistry
2010

Acknowledgements

At the Woodruff Memorial Research Building on Emory's campus, there is a memorial to the building's namesake which has an embossed bust and impressed into the wall is the prayer: "Lighten our darkness we beseech Thee, O Lord". Scientific research is asking God to show His laws in constant, measurable, and certain terms. To this end, I give the greatest acknowledgement to my Lord and Lady for Their aid and guidance during this time and throughout my life. I would truly be in no good way without them.

After those two everyone else is really insignificant.

The most important of the "everyone else" is my mother, Mary Ann Anderson. Without her of the love and support I would have lost my mind the first week.

From among my various mentors I thank the Chemistry faculty at Georgia Southern University, and especially Dr. James M. LoBue for the numerous hours I have robbed him by "jawin' away" and for his being the voice of reason in my academic life (even if I don't always listen and end up regretting it). I would also like to thank Ms. Tommy Evans and Ms. Lynn Brinson, my high school chemistry and calculus teachers for giving me my first real glimpse into the beautiful world that is science.

Lastly I thank my committee members and group mates for their contributions to my life and to the ideas in this work. It has certainly been an interesting two years.

Abstract

Calculations of Prebiotic Molecules Formed from O(^{1}D) Insertion Reactions

By Thomas Anderson

This work explores the stationary points on the potential energy surface for the reactive organic molecules methanediol, methoxymethanol, and aminomethanol. These molecules are predicted by astrochemical models to be the small molecular precursors to larger, biologically-relevant molecules such as sugars and amino acids in interstellar environments. These three molecules are highly unstable and therefore very short-lived under regular laboratory conditions. Yet many such molecules are present in interstellar clouds, often at high abundance because their lifetimes are significantly increased at the low pressures and temperatures of interstellar environments. To identify a molecule in space, a rotational spectrum must be taken in the laboratory and compared to observational spectra. Due to the reactivity and instability of these prebiotic precursors, however, the gas phase spectra are not easily obtained, and efficient laboratory production mechanisms must be explored. O(^{1}D) insertion reactions into C-H bonds of stable organic molecular precursors are one possible production route for these molecules because these reactions are highly exothermic, and therefore highly efficient. To examine the feasibility of such reactions for laboratory production of these molecules, the energies and structures of the singlet and triplet state minima and transition states for these three molecules were calculated at the MP2/Aug-cc-pVTZ level of theory. These results will serve as a starting-point for higher-level calculations of the full potential energy surface. In addition to the target molecules, the starting material for each insertion reaction as well as other potential molecular products were investigated.

Table of Contents

List of Figures

List of Tables

Chapter 1

Background

1.1 Introduction

One of the leading theories for the origin of life is that prebiotic materials from the interstellar medium may have been deposited onto early Earth by impacts of comets, meteorites, and interplanetary dust particles [1, 2]. The search for the simplest biologically-relevant amino acid, glycine, in the interstellar medium has been in progress since the late 1970s, and no definitive results have been obtained [2]. Amino acids such as glycine and other prebiotic molecules such as sugars are predicted to form in gas-phase ion-molecule reactions in interstellar clouds [3]. The unique physical environment in interstellar clouds allows for terrestrially-unstable or reactive species to be important and observable in astrochemical processes [4, 5], and such species are predicted to be key reaction intermediates leading to sugars and amino acids [3]. Searches for these precursors, rather than the larger and more difficult to detect biomolecules, offers an alternate course in the search for biologically-relevant molecules in the interstellar medium.

Before such searches can be performed, laboratory spectra are required for the major chemical precursors to amino acids and sugars in interstellar clouds. Electronic structure calculations offer the information necessary to guide these laboratory spectral studies. The purpose of the work described here is to examine the energetics and formation of the prebiotic molecules methanediol ($HOCH_2OH$), methoxymethanol

(CH_3OCH_2OH), and aminomethanol (NH_2CH_2OH) through ab initio calculations of the stationary points on their potential energy surfaces. According to Garrod et al., [3] these molecules are predicted to form in interstellar ices and serve as precursor molecules in the gas-phase formation of prebiotic materials. However, given the reactivity and instability of these molecules under normal laboratory conditions, an efficient, gas-phase chemical formation mechanism is required before laboratory studies can be conducted. The proposed mechanism for creating these molecules is $O(^1D)$ insertion into the C-H bonds of stable organic precursors. The following reactions are proposed:

$CH_3OH + O(^1D) \rightarrow CH_2(OH)_2$ Equation 1

$CH_3OCH_3 + O(^1D) \rightarrow CH_3OCH_2OH$ Equation 2

$H_2NCH_3 + O(^1D) \rightarrow H_2NCH_2OH$ Equation 3

1.2 Atomic Oxygen

$O(^1D)$ is an electronically-excited form of atomic oxygen that undergoes exothermic insertion reactions into C-H bonds. $O(^1D)$ has therefore been used extensively in molecular beam experiments to study the nature of simple molecular processes that are relevant to environmental and atmospheric processes [6 – 13].

$O(^1D)$ is the first electronically excited state of oxygen, while $O(^3P)$ is the ground state. The transition to the triplet ground state from the singlet excited state is 15867.862 cm^{-1} [14, 15], but it is spin-forbidden. While $O(^1D)$ is highly reactive, it is also long-lived, with a relaxation time of about 2.5 minutes [16]. When $O(^1D)$ reacts with organic molecules, it has been shown to insert into C-H bonds. These insertion reactions are

highly exothermic, and generally the unquenched insertion products quickly degrade, primarily forming OH as a product [17 - 19]. At low temperatures, the insertion products can be isolated for extended time periods for study [20]. $O(^1D)$ insertion reactions have mainly been used to study the insertion reaction dynamics of atmospheric species. These reactions hold the potential for a new approach to forming unstable reaction intermediates in high yield, especially organic molecules that might be important in interstellar processes.

$O(^1D)$ is primarily produced from photolysis of simple oxygen containing gases such as CO_2, NO_2, N_2O, O_3 and O_2. Each of these molecules dissociates in the ultraviolet region between 100 – 250 nm [21 – 23]. The ultraviolet dissociation of these molecules can produce many other species aside from $O(^1D)$. O_2 produces both states of atomic oxygen in a ^1D:^3P ratio of 40:60 at 132.7 nm, although $O(^1D)$ has been found to be up to 70% of the product at certain photolysis wavelengths [24]. Molecules with multiple oxygen atoms can produce both $O(^1D)$ and $O(^3P)$ simultaneously. Examples of this are NO_2 and O_3. The three channels for NO_2 dissociation [26] are:

$$NO_2 + h\nu \rightarrow O(^3P) + NO(^2\Pi) \quad \lambda < 398 \text{ nm} \qquad \text{Equation 4}$$

$$NO_2 + h\nu \rightarrow O(^1D) + NO(^2\Pi) \quad \lambda < 244 \text{ nm} \qquad \text{Equation 5}$$

$$NO_2 + h\nu \rightarrow N(^4S) + O_2(^3\Sigma^-) \quad \lambda < 275 \text{ nm} \qquad \text{Equation 6}$$

The products of ozone dissociation are shown with their threshold wavelengths in Table 1.01.

Table 1.01. Thermochemical Threshold Wavelengths (nm) for Photodissociation Pathways of O_3.

	$O_2(X^3\Sigma_g^-)$	$O_2(a^1\Delta_g)$	$O_2(b^1\Sigma_g^+)$	$O_2(A^3\Sigma_u^+)$	$O_2(B^3\Sigma_u^-)$	$2O(^3P)$*
$O(^3P)$	1180	590	460	230	170	198
$O(^1D)$	410	310	260	167	150	
$O(^1S)$	234	196	179	129	108	

*Taken from Reference [i.07], in which Reference [i.19] was cited for the data

With the high likelihood of producing $O(^3P)$ from photodissociation or $O(^1D)$ relaxation, there is a possibility of reactions between the ground state atoms and molecules producing triplet states [27 - 30]. Much like $O(^1D)$, $O(^3P)$ is also very relevant in atmospheric reactions, and its reaction dynamics have been extensively studied in molecular beam experiments [31 - 34]. Where singlet oxygen inserts into the C-H bonds of organic molecules, $O(^3P)$ commonly abstracts hydrogens, forming OH [35 - 37].

1.3 Methanediol and Methoxymethanol

Methylene glycol, also known as methanediol ($CH_2(OH)_2$), and methyl hemiformal, also known as methoxymethanol (CH_3OCH_2OH), both form from the hydrolysation of formaldehyde in solution [38 - 50]. Formaldehyde is important in environmental studies [51 - 53] and for industrial production of resins and acetylene chemicals [54]. Formaldehyde is also able to form prebiotic materials such as carbohydrates and amino acids [55 - 58], converting to methanediol and methoxymethanol as intermediate structures during these reaction pathways. Formaldehyde was first identified in space in 1969 [59]. According to Garrod et. al. [3], methanediol is predicted to form in the interstellar medium from radical-radical reactions

involving OH and CH_2OH produced from methanol photodissociation. Likewise, methoxymethanol forms from reaction of two methanol photodissociation products, CH_3O and CH_2OH. In previous experiments, methanediol has been produced by hydrolysis of dichloromethane [60]. Likewise, methoxymethanol has been produced in the liquid phase by methanol photolysis with a TiO_2 catalyst [62] and in the gas phase by irradiating methanol with a carbon dioxide laser [61]. Methanol and dimethyl ether reactions with $O(^1D)$ have also produced methanediol [63] and methoxymethanol [64] in cryogenic matrices.

1.4 Aminomethanol and N-Methylhydroxylamine

Aminomethanol (H_2NCH_2OH) is formed by reaction of ammonia and formaldehyde in the liquid phase [65, 66]. Aminomethanol further reacts to form hexamethylenetetramine which is used in the production of explosives and resins [54]. Aminomethanol spectra have been taken in the infrared on gas mixtures deposited onto a 10 K metal surface. When compared to astronomical observational data the signatures were indistinguishable due to the high number of peaks within the frequency range [67].

A major constitutional isomer of aminomethanol, N-methylhydroxylamine (CH_2NHOH) is stable in the solid form in a complex with hydrochloride. With the stability of N-methylhydroxylamine, there is a need to compare the energies of aminomethanol and N-methylhydroxylamine and fully understand the energy differences between the two.

1.5 Calculations

The calculations performed on methanediol, methoxymethanol, aminomethanol, and N-methylhydroxylamine will be used to find the geometry of all possible stationary points and transition structures of these molecules. The calculated rotational constants and dipole moments can be used in assigning the rotational spectra. The energies can be used to construct potential energy surfaces for the molecules. The singlet and triplet surfaces of each molecule are needed to determine possible geometries and energies in which singlet molecules could cross into the triplet system or vice versa. These calculations are needed to fully understand and predict the mechanisms of the formation of these prebiotic precursors.

Chapter 2

$O(^1D)$ Insertion Reaction Starting Material

2.1 Introduction

In order to find the energy released by forming methanediol, methoxymethanol, and aminomethanol from organic molecules and atomic oxygen, the energies of the organic starting materials are needed to compare with the final singlet and triplet structures of the target molecules.

The optimizations of the starting materials were performed at the Møller-Plesset, MP2 level of perturbation theory [68, 69] with the augmented Dunning correlation consistent triple zeta basis set, Aug-cc-pVTZ [70, 71], using the Gaussian 09 software package [72]. The initial structure input for each molecule was determined using the ACD/ChemSketch software [74]. The geometry optimization function within this program uses a molecular mechanics force field, modified from CHARMM parameterization [73]. The geometries were then used as the input to Gaussian, and individually optimized at increasing levels of theory up to the MP2/Aug-cc-pVTZ level. The specific calculation details and the results of these optimizations are given below for each molecule.

2.2 Atomic Oxygen

Due to the multi-reference nature of $O(^1D)$, an $O(^3P)$ MP2 calculation is used to compute the $O(^1D)$ energy. A MP2/Aug-cc-pVTZ level calculation on a triplet multiplicity atomic oxygen yielded an energy of -74.8610509 hartrees, (-46976.01 kcal/mol).

According to the NIST Atomic Spectral Database the transition energy between $O(^1D)$ and $O(^3P)$ is 15867.862 cm^{-1} (45.34 kcal/mol) [14, 15]. Using the oxygen transition and $O(^3P)$ energy, the $O(^1D)$ energy is calculated to be -46930.66 kcal/mol. A summary of the energy of atomic oxygen is found in Table 2.01.

Table 2.01. Energy of atomic oxygen.

		Energy
Gaussian Calculation	$O(^3P)$	-46976.01 kcal/mol
NIST[14, 15]	$O(^3P) \rightarrow O(^1D)$	45.34 kcal/mol
	$O(^1D)$	-46930.68 kcal/mol

2.3 Methanol

The methanol structure optimization was performed at the MP2 level of theory with the following Pople and Dunning basis sets: 6-311+G(2d,p), 6-311+G(2df,pd), cc-pVTZ, 6-311G(3d2f,3pd), 6-311G(3d2f,3p2d), Aug-cc-pVTZ. The spectral parameters of methanol are listed in Table 2.02 and the final structure is shown in Figure 2.01.

Table 2.02. Spectral parameters for methanol calculated using MP2 perturbation theory and Aug-cc-pVTZ basis set and comparative experimental values.

Parameter	Methanol	Experimental [75]
Energy Relative to Methanediol	47150.46 kcal/mol	
A	128.6271561 GHz	127.6219411(400) GHz
B	24.7600271 GHz	24.69323850(12000) GHz
C	23.8937795 GHz	23.75685126(12000) GHz
μ_x	-0.9449 D	
μ_y	-1.5465 D	
μ_z	0.0000 D	

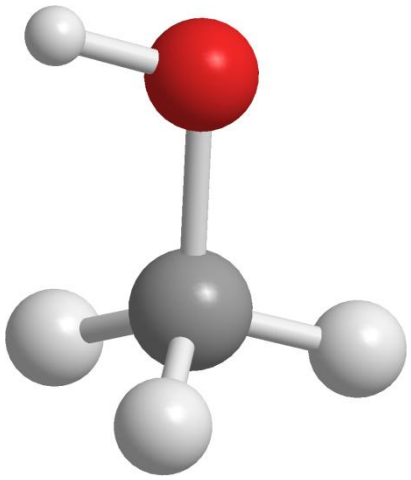

Figure 2.01. MP2/Aug-cc-pVTZ optimized structure of methanol.

These calculations give agreement on the order of 0.067 - 1.005 GHz with experimentally-measured values of the rotational constants [75]. Further structural information on methanol can be found in Appendix A.

2.4 Dimethyl Ether

The dimethyl ether structure optimization was performed at the MP2 level of theory with the following Pople and Dunning basis sets: 6-311+G(2d,p), 6-311+G(2df,pd), cc-pVTZ, 6-311G(3d2f,3pd), 6-311G(3d2f,3p2d), Aug-cc-pVTZ. The spectral parameters of dimethyl ether are listed in Table 2.03 and the final structure is shown in Figure 2.02.

Table 2.03. Spectral parameters for dimethyl ether calculated using MP2 perturbation theory and Aug-cc-pVTZ basis set and comparative experimental values.

Parameter	Dimethyl Ether	Experimental [76]
Energy Relative to Methoxymethanol	47149.49 kcal/mol	
A	38.5508496 GHz	38.7893953(109) GHz
B	10.1982683 GHz	10.0565381(29) GHz
C	8.9784426 GHz	8.88680566(278) GHz
μ_x	0.0000 D	
μ_y	0.0000 D	
μ_z	-1.4864 D	

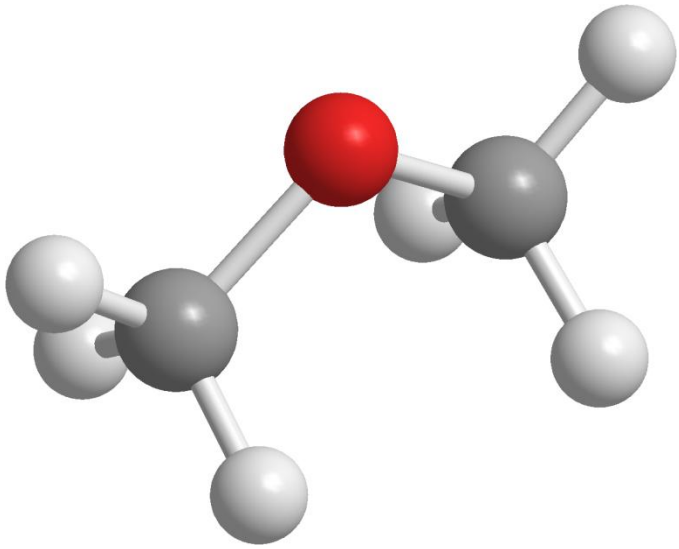

Figure 2.02. MP2/Aug-cc-pVTZ optimized structure of dimethyl ether.

These calculations give agreement with experimentally-determined values to within 0.24 GHz [76]. Further structural information on dimethyl ether can be found in Appendix A.

2.5 Methylamine

The methylamine structure optimization was performed at the MP2 level of theory with the following Pople and Dunning basis sets: 6-311+G(2d,p), 6-311+G(2df,pd), cc-pVTZ, 6-311G(3d2f,3pd), 6-311G(3d2f,3p2d), Aug-cc-pVTZ. The spectral parameters of methylamine are listed in Table 2.04 and the final structure is shown in Figure 2.03.

Table 2.04. Spectral parameters for methylamine calculated using MP2 perturbation theory and Aug-cc-pVTZ basis set and comparative experimental values.

Parameter	Methylamine	Experimental [77]
Energy Relative to Aminomethanol	47147.434911 kcal/mol	
A	104.0972245 GHz	103.1557485(44) GHz
B	22.8129272 GHz	22.16936633(30) GHz
C	21.9331791 GHz	21.29148937(24) GHz
μ_x	-1.3423 D	
μ_y	0.4281 D	
μ_z	0.0000 D	

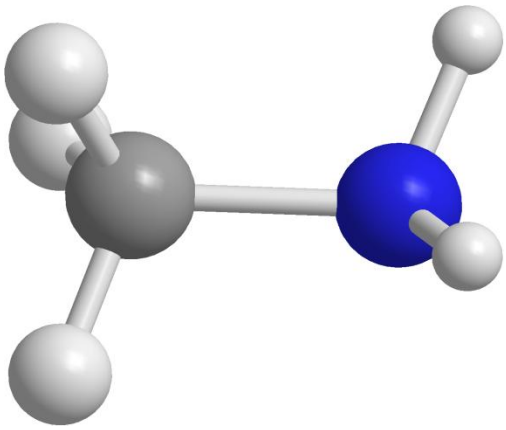

Figure 2.03. MP2/Aug-cc-pVTZ optimized structure of methylamine.

Experimentally determined rotational constants [77] give agreement with these calculated values to within 1.0 GHz. Further structural information on methylamine can be found in Appendix A.

Chapter 3

Singlet State Product Optimizations

3.1 Introductions

The singlet state optimizations of the product molecules were performed at the Møller-Plesset, MP2 level of perturbation theory [68] [69] with the augmented Dunning correlation consistent triple zeta basis set, Aug-cc-pVTZ [70] [71], using the Gaussian 09 software package [72]. The initial structure input for each molecule was determined using the ACD/ChemSketch software [74]. The geometry optimization function within this program uses a molecular mechanics force field, modified from CHARMM parameterization [73]. Using this simple structure output, the functional groups were rotated to give the starting geometries for finding the structural minima. These different geometries were then used as the input to Gaussian, and individually optimized at increasing levels of theory up to the MP2/Aug-cc-pVTZ level.

Transition states were determined at the MP2/Aug-cc-pVTZ level using the Synchronous Transit-Guided Quasi-Newton Method [78]. The Gaussian 09 functions used were QST2, which formulates a starting point from just the two stable structures, and QST3, which requires an additional input structure. The specific calculation details and the results of these optimizations are given below for each molecule.

3.2 Methanediol

Seven initial geometries of methanediol were selected to be optimized. They were obtained by rotating the torsion angles of the two hydroxyl groups in 90° increments. The optimization calculations on each geometry were performed in the following order: B3LYP/6-311+G**, B3LYP/6-311+G(2d,p), MP2/6-311+G(2d,p), MP2/6-311+G(2df,pd), MP2/cc-pVTZ, and MP2/Aug-cc-pVTZ. The seven geometries converged to two distinct geometries after this series of six calculations. The ground state geometry showed close agreement with previous lower level computations in the angles and hydroxyl orientation [79, 80]. The ground state hydroxyl conformer has H-O-C-O dihedral angles of -68° where as the second conformer has dihedral angles of ±78°. Figure 3.01 shows the resulting minimum energy structures of the two conformers and Table 3.01 shows their relative energies, rotational constants, and dipole moments. Further structural information on this molecule can be found in Appendix B.

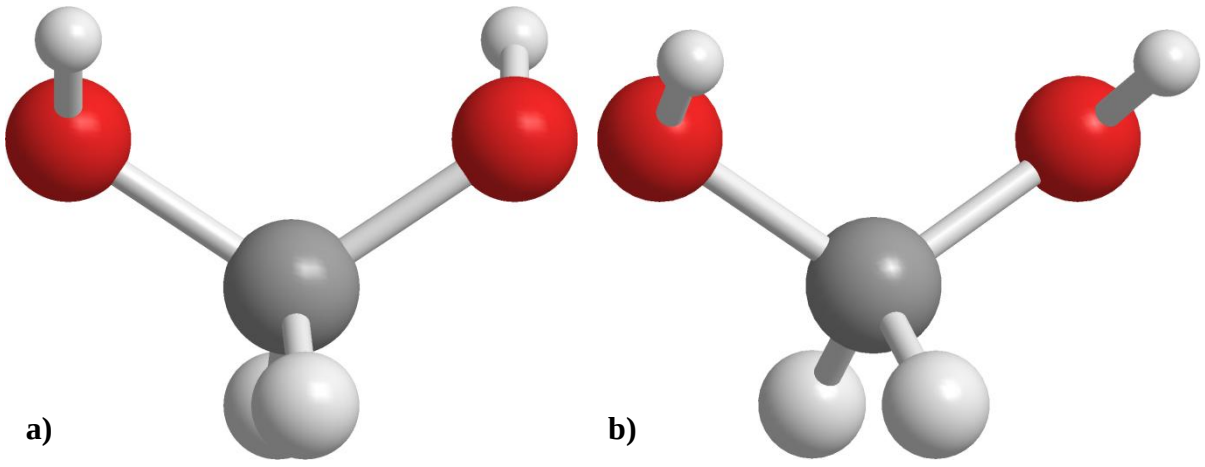

Figure 3.01. Structures of the two methanediol singlet conformations: a) ground state conformer having OH groups in opposing directions giving an approximate C_{2v} geometry; b) conformer closely resembling a C_s symmetry due to OH groups oriented in same direction.

Table 3.01. Spectral parameters for the two singlet conformers of methanediol calculated in Gaussian 09 using MP2 perturbation theory and Aug-cc-pVTZ basis set.

Parameter	Conformer a	Conformer b
Energy	0 kcal/mol	2.68 kcal/mol
A	41.8847600 GHz	43.3730609 GHz
B	10.1983735 GHz	9.9012179 GHz
C	9.0371184 GHz	8.9059764 GHz
μ_x	0.0000 D	0.0000 D
μ_y	0.0000 D	0.2802 D
μ_z	0.0290 D	-2.9009 D

The transition states corresponding to the internal motion of the OH group between these two geometries were determined using the QST3 function at MP2/Aug-cc-pVTZ computation level. The transition state structures are shown in Figure 3.02. A diagram of the relative energies of the minima and two transition states is shown in Figure 3.03.

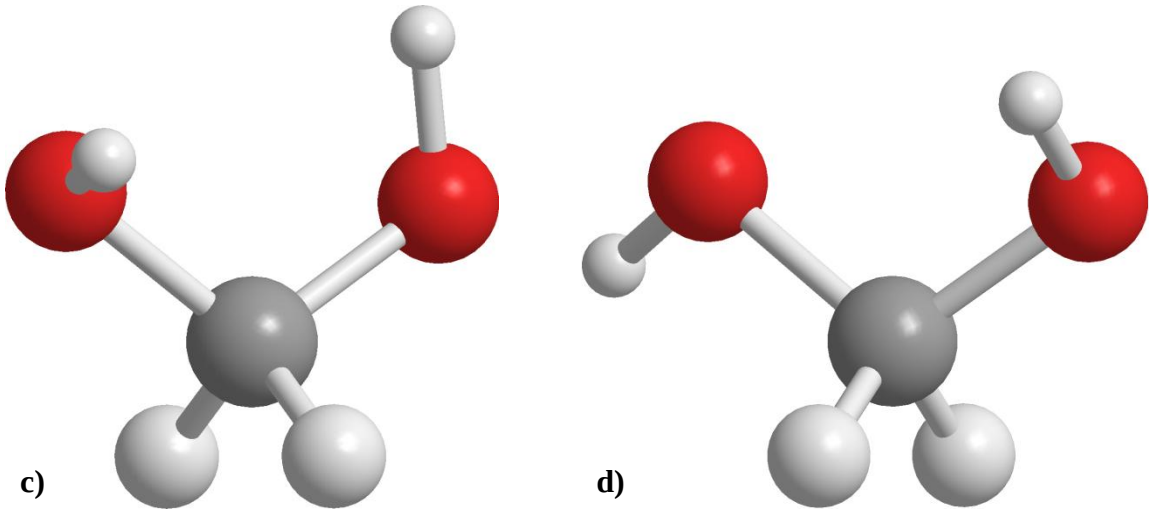

Figure 3.02. Transition states of methanediol at the following relative energies: c) 3.61 kcal/mol; d) 3.81 kcal/mol.

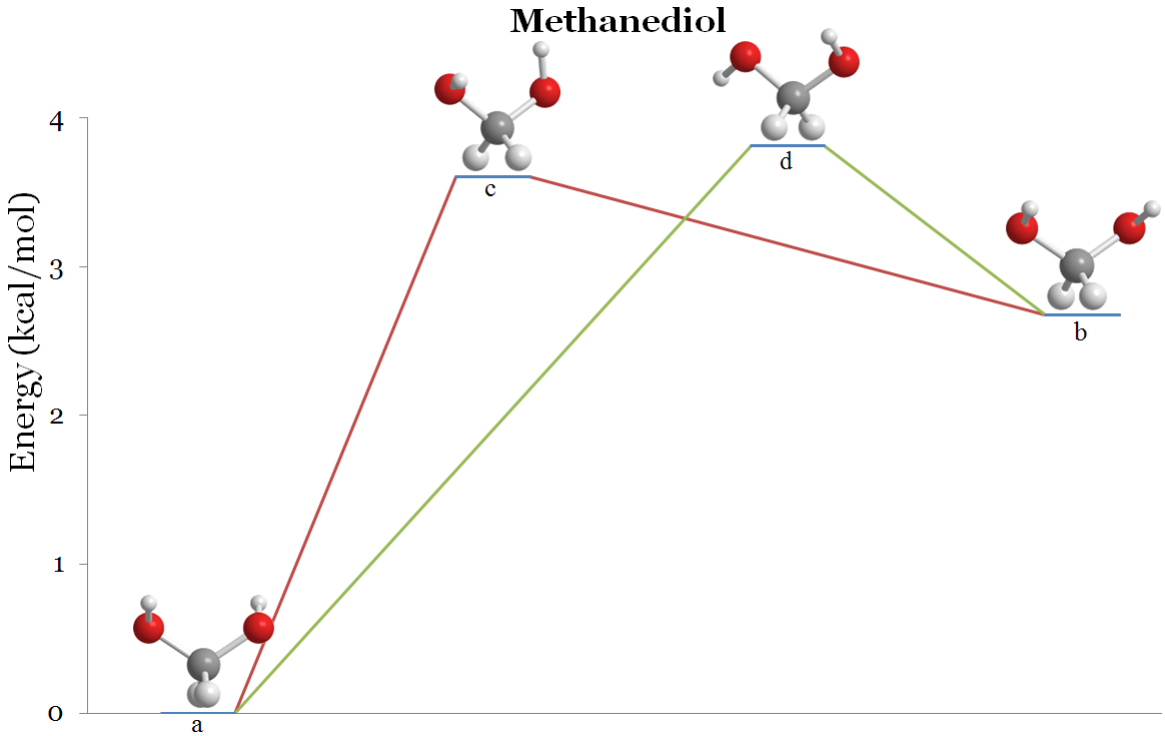

Figure 3.03. Relative energies of the stationary points for singlet methanediol. Labels correspond to the geometries shown in Figures 3.01. and 3.02.

When compared to its starting materials of methanol and O(^{1}D), there are 219.78 kcal/mol of exothermic energy to the ground state of methoxymethanol. Further structural information for the stationary points and transition states can be found in Appendix B.

3.3 Methoxymethanol

The conformations of methoxymethanol were probed using 24 initial geometries obtained by rotating the methyl and hydroxyl groups in 45° increments. All twenty four geometries were optimized at the following levels: B3LYP/6-311G**, B3LYP/6-311++G**, MP2/6-311++G**, MP2/6-311++G(2df,2pd), and MP2/cc-pVTZ. The resulting structures and energies were analyzed and duplicate structures eliminated so as to reduce the number of computations required at the MP2/Aug-cc-pVTZ level.

Ultimately only four distinct geometries remained. These four were optimized at the MP2/Aug-cc-pVTZ level. Calculations from Wrobel et al. [81] show three similar structures for stationary points; the fourth geometry found in this calculation is similar to a transition state included in this previous work. A frequency calculation at MP2/Aug-cc-pVTZ level confirmed Wrobel's conclusions that the fourth structure has a single negative frequency and therefore is a transition state. The spectral parameters of the three conformers are listed in Table 3.02 and the structures are shown in Figure 3.04. Further structural information on this molecule can be found in Appendix B

Table 3.02. Spectral parameters for the three singlet conformers of methoxymethanol calculated using MP2 perturbation theory and Aug-cc-pVTZ basis set.

Parameter	Conformer a	Conformer b	Conformer c
Energy	0 kcal/mol	2.05 kcal/mol	2.64 kcal/mol
A	17.1548902 GHz	17.0926945 GHz	32.5310742 GHz
B	5.6237150 GHz	5.6688880 GHz	4.3667976 GHz
C	4.8517481 GHz	4.7971284 GHz	4.0866261 GHz
μ_x	-0.2135 D	0.8624 D	1.5855 D
μ_y	0.1003 D	1.2271 D	1.0069 D
μ_z	-0.1162 D	2.1883 D	1.4187 D

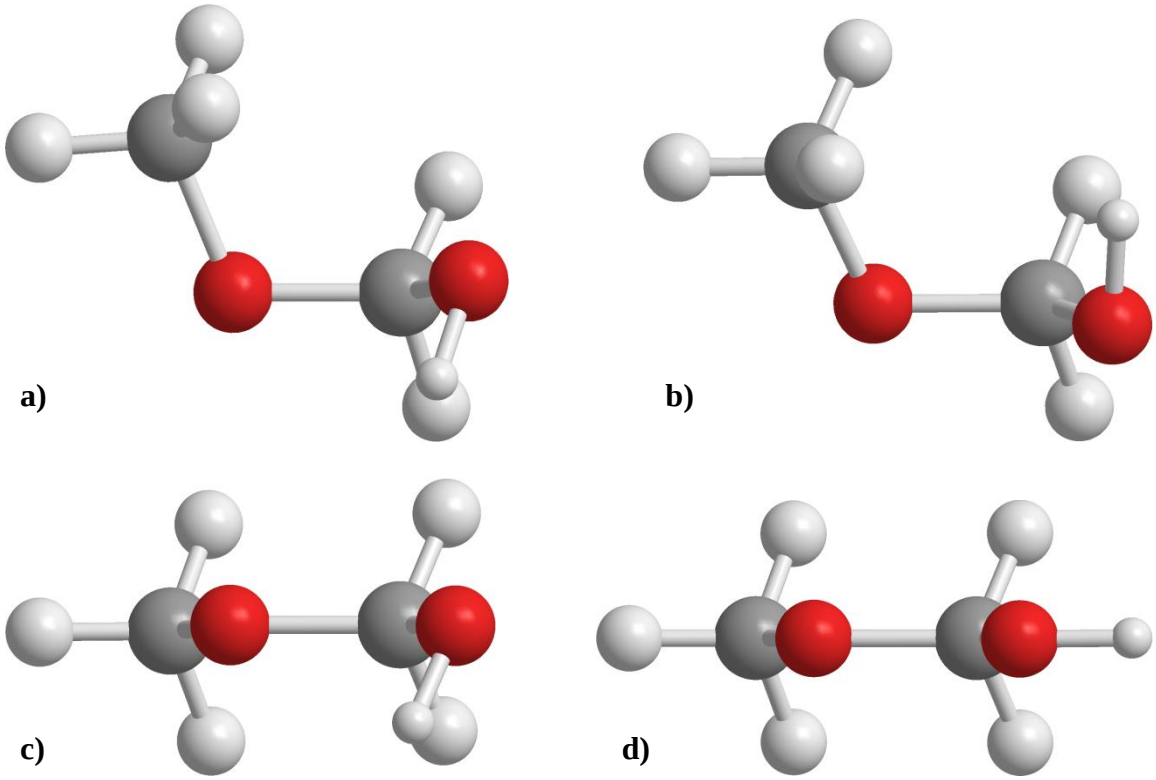

Figure 3.04. Structures of the three methoxymethanol singlet conformations at the following relative energies: a) ground state conformer; b) 2.05 kcal/mol; c) 2.64 kcal/mol; d) transition state at 6.42 kcal/mol.

Additional transition states between the three stable structures were found using the QST2 function. The structures of the transition states are shown in Figure 3.05 and a plot of the relative energies is shown in Figure 3.06.

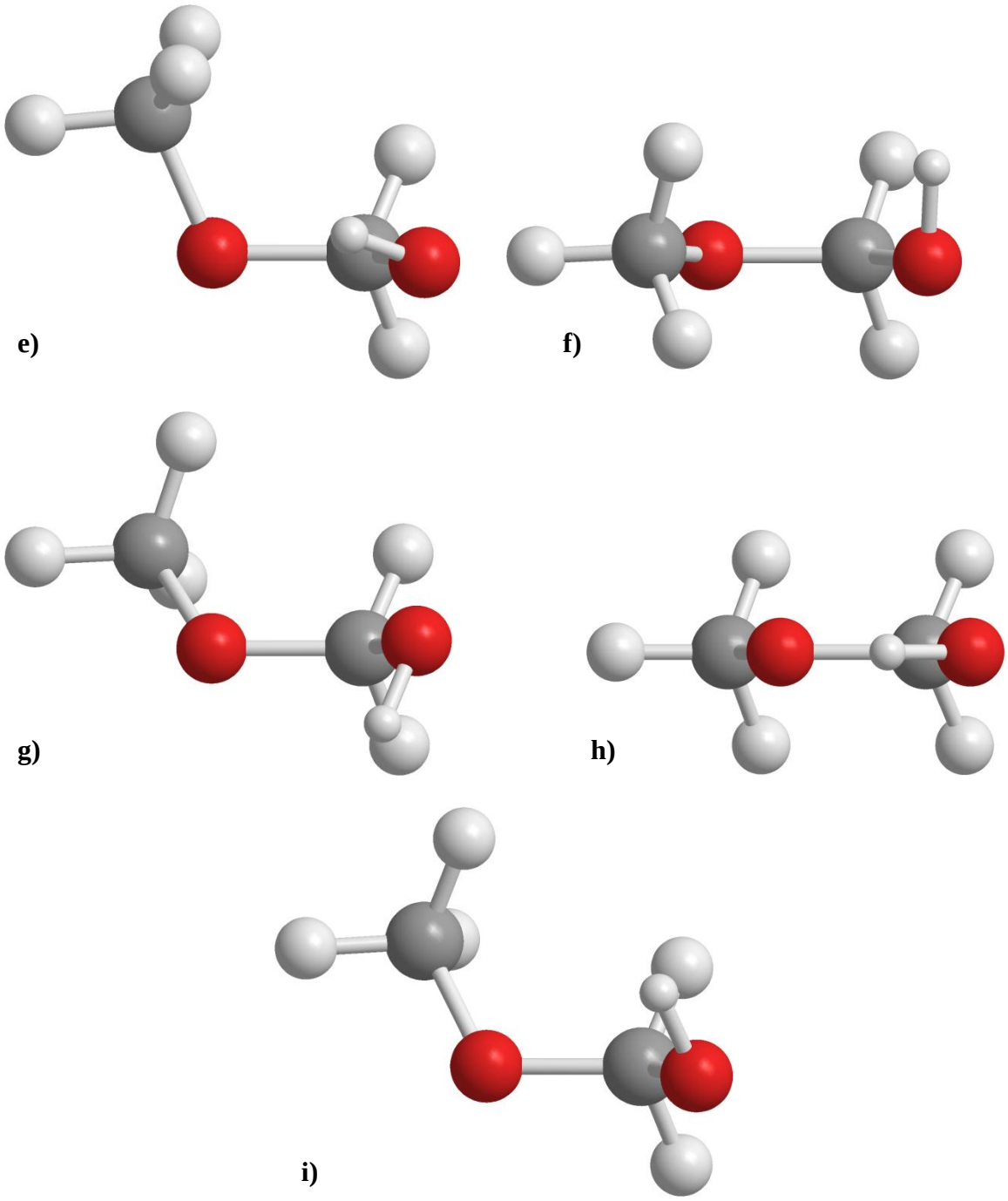

Figure 3.05. Structures of the five methoxymethanol singlet transition states determined by QST2 optimization: e) 4.20 kcal/mol transition state between the a and b structures; f) 7.13 kcal/mol transition state between the a and b structures; g) 4.08 kcal/mol transition state between the a and e structures; h) 4.05 kcal/mol transition state between the b and e structures; i) 4.38 kcal/mol transition state between the b and e structures.

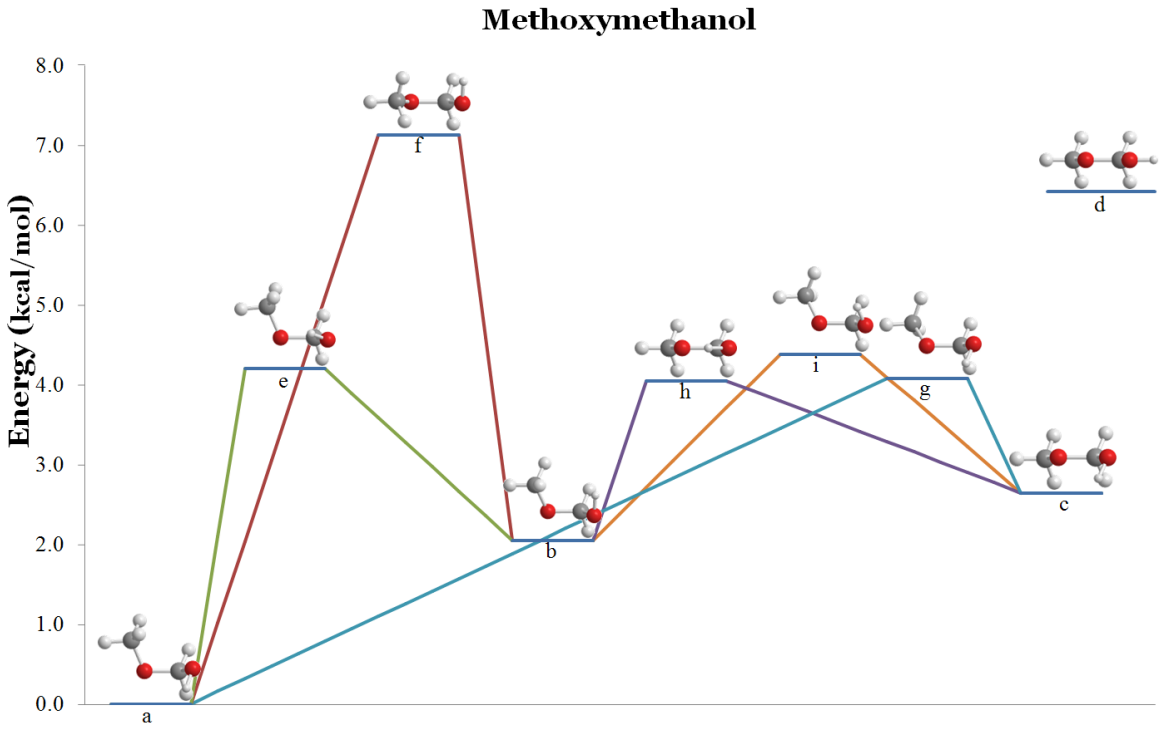

Figure 3.06. Relative energies of the stationary points for singlet methoxymethanol. Labels correspond to the geometries shown in Figures 3.04 and 3.05.

Wrobel et al. predicts the d transition structure in Figure 3.04 and e and f in Figure 3.05. This previous study does not predict the other three transition states found in our work. To find these additional transition states g, h, and i, the O-C-O-C and O-C-O-H torsion angles were used to predict structures used in QST3 calculations.

When compared to the starting materials of dimethylether and O(^{1}D), there are 218.84 kcal/mol of energy released upon formation of the ground state of methoxymethanol. Further structural information on the methoxymethanol stationary points and transition states can be found in Appendix B.

3.4 Aminomethanol

The conformations of aminomethanol were probed using ten initial geometries obtained by rotating the hydroxyl group and the amine hydrogens in 90° increments. The geometries were optimized at the following levels: B3LYP/6-311+G(d,p), B3LYP/6-311+G(2d,p), MP2/6-311+G(2d,p, MP2/6-311+G(2df,pd), MP2/cc-pVTZ, and MP2/Aug-cc-pVTZ. The spectral parameters of the four stable conformers are listed in Table 3.03 and the structures are shown in Figure 3.07

Table 3.03. Spectral parameters for the four singlet conformers of aminomethanol calculated using MP2 perturbation theory and Aug-cc-pVTZ basis set.

Parameter	Conformer a	Conformer b	Conformer c	Conformer d
Energy	0 kcal/mol	0.29 kcal/mol	0.78 kcal/mol	4.36 kcal/mol
A	38.695424 GHz	38.952998 GHz	38.996584 GHz	40.766228 GHz
B	9.545985 GHz	9.865754 GHz	9.897697 GHz	9.835920 GHz
C	8.586625 GHz	8.665098 GHz	8.688179 GHz	8.614444 GHz
μ_x	0.3832 D	0.9423 D	-2.0000 D	-0.4030 D
μ_y	-0.9982 D	0.7508 D	0.6866 D	2.3996 D
μ_z	1.3380 D	0.0000 D	-0.2152 D	1.6783 D

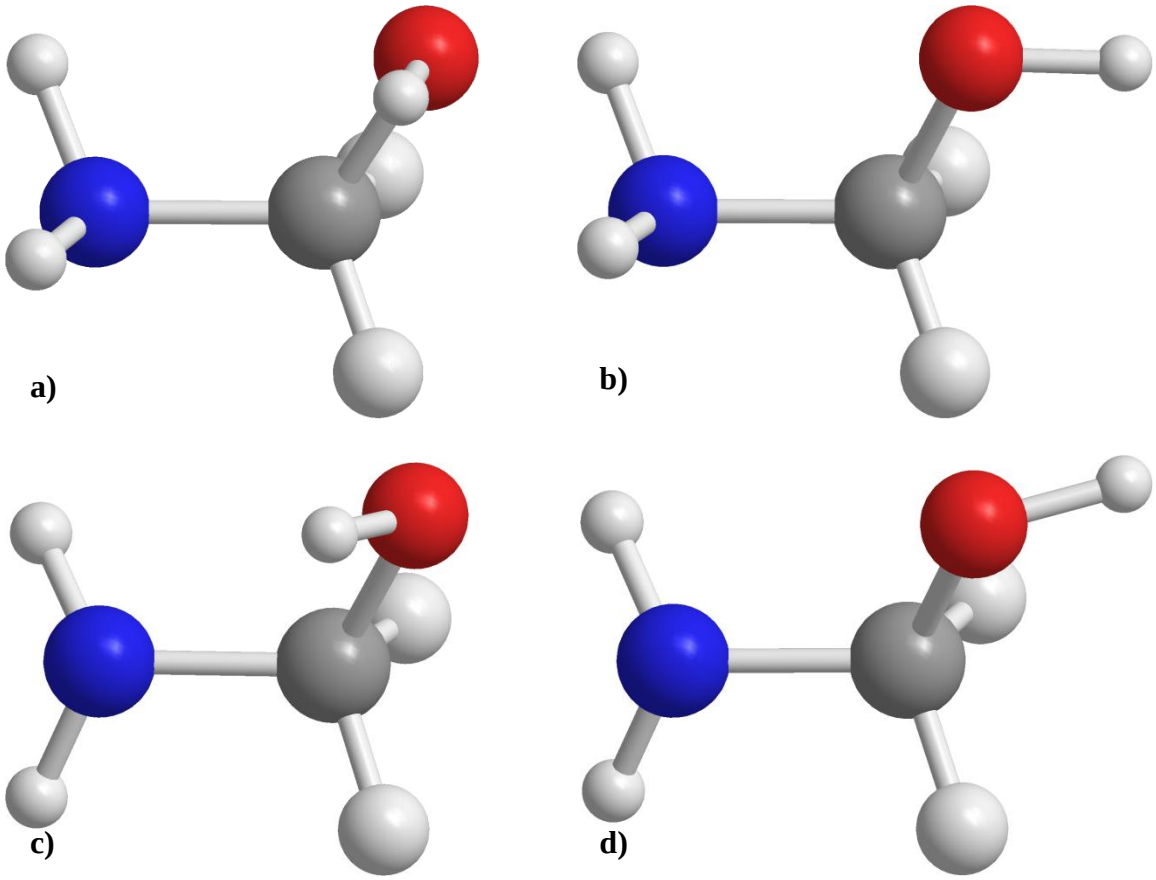

Figure 3.07. Structures of the four aminomethanol singlet conformations: a) ground state conformer; b) 0.29 kcal/mol; c) 0.78 kcal/mol; d) 4.36 kcal/mol.

Using the QST3 function four transition states were determined and are shown in Figure 3.08. An energy diagram is shown in Figure 3.09.

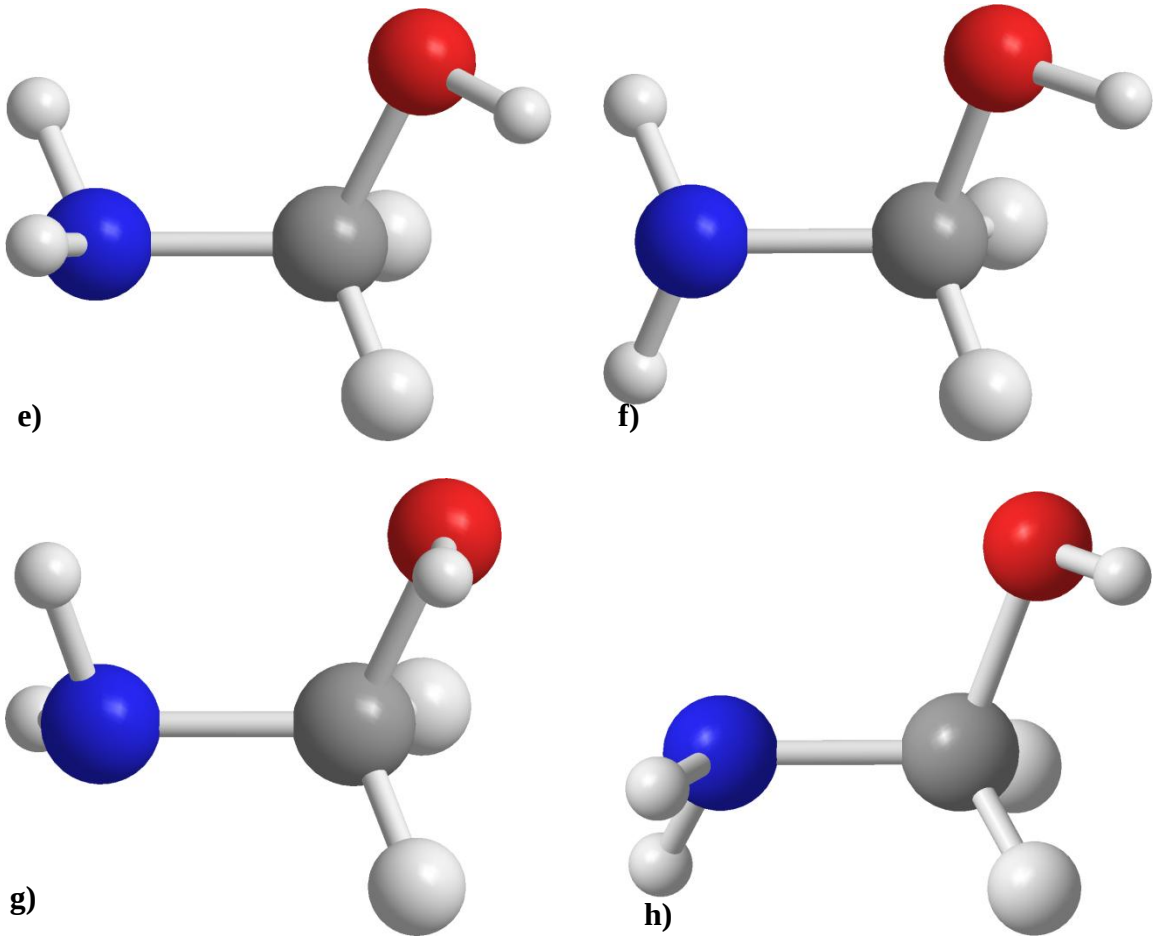

Figure 3.08. Structures of the four aminomethanol singlet transition states determined by QST3 optimization: e) transition state between the a and b states, having a 0.93 kcal/mol barrier; f) transition state between the a and d and the c and d states having a 5.36 kcal/mol barrier; g) transition state between the b and c states having a 4.96 kcal/mol barrier; h) transition state between the c and d states having a 4.73 kcal/mol barrier.

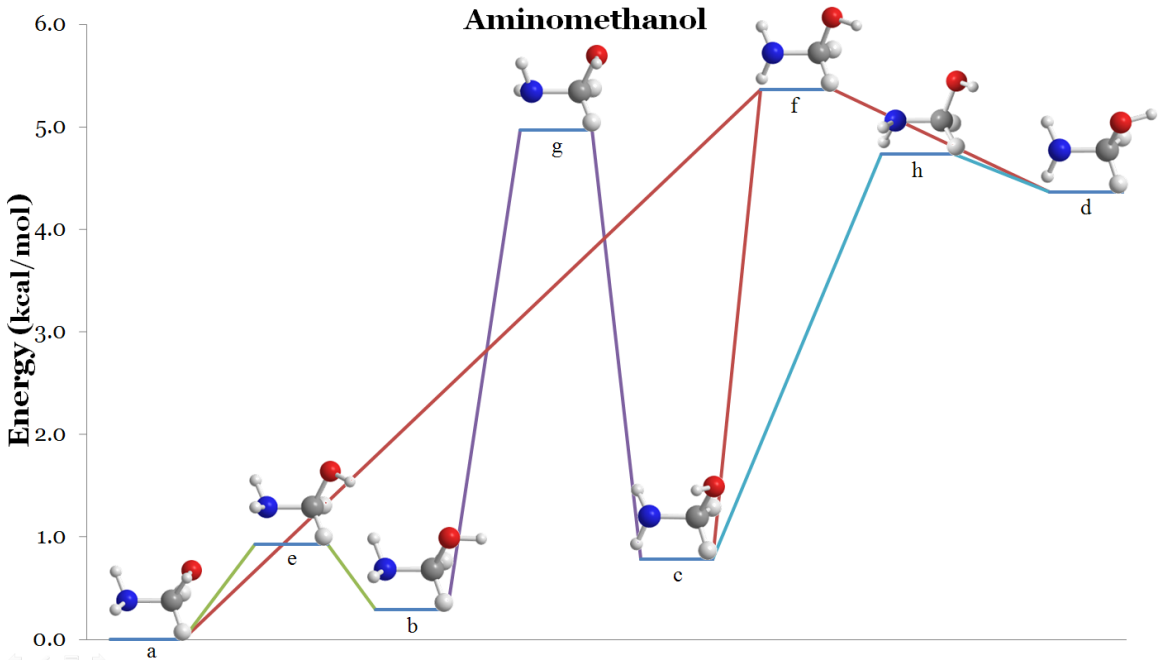

Figure 3.09. Relative energies of the stationary points for singlet aminomethanol. Labels correspond to the geometries shown in Figures 3.07 and 3.08.

Further structural information on the stationary points can be found in Appendix B. The potential energy surfaces produced by El-Issa and Budeir [72] guided a further search for transition states but no additional states were found. By comparison to their potential energy surface, this work indicates an additional stationary point but cannot identify two of the six transition structures found in the El-Issa surface [72].

3.5 N-Methylhydroxylamine

The conformations of N-methylhydroxylamine were probed using four initial geometries obtained by rotating the hydroxyl group by 90° increments. The geometries were optimized at the following levels: B3LYP/6-311+G(d,p), B3LYP/6-311+G(2d,p), MP2/6-311+G(2d,p, MP2/6-311+G(2df,pd), MP2/cc-pVTZ, and MP2/Aug-cc-pVTZ.

The spectral parameters of the three conformers are listed in Table 3.04 and the structures are shown in Figure 3.10.

Table 3.04. Spectral parameters for the singlet conformers of N-methylhydroxylamine calculated using MP2 perturbation theory and Aug-cc-pVTZ basis set.

Parameter	Conformer a	Conformer b	Experimental [83]
Energy	0 kcal/mol	3.57 kcal/mol	
Energy Relative to Aminomethanol	38.37 kcal/mol	41.94 kcal/mol	
A	39.1249262 GHz	38.5307458 GHz	38.930771 GHz
B	10.0315604 GHz	10.1680157 GHz	9.939607 GHz
C	8.7768030 GHz	8.8333440 GHz	8.690716 GHz
μ_x	-0.1303 D	1.7156 D	
μ_y	0.4704 D	-0.6803 D	
μ_z	0.6609 D	2.4515 D	

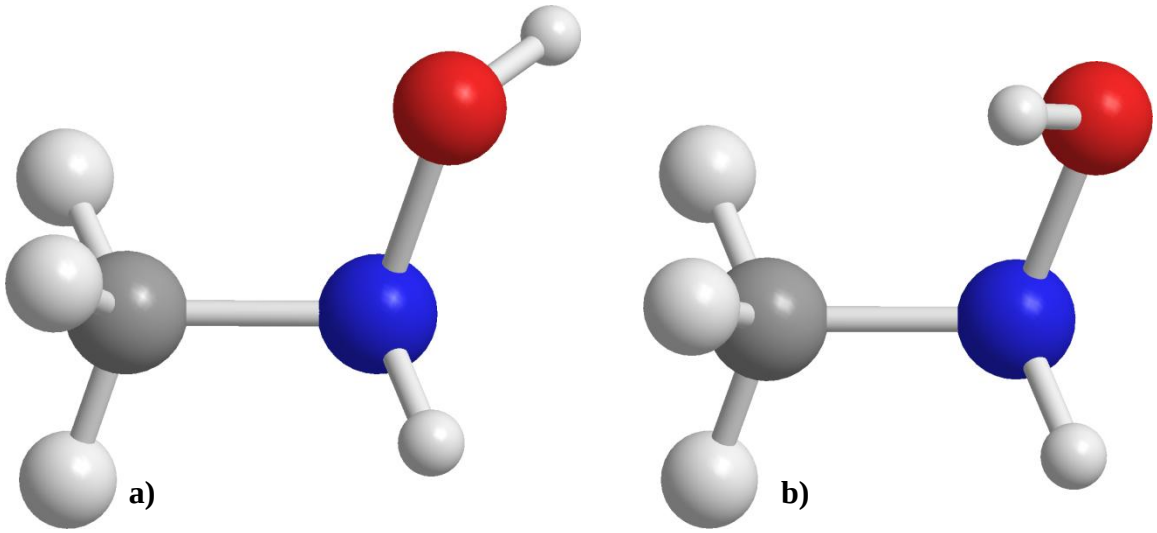

Figure 3.10. The two stable structures of N-methylhydroxylamine singlet conformations.

Experimental data on N-methylhydroxylamine shows agreement with the calculated rotational constants to within 0.20 GHz [83]. The microwave spectra also suggest a high barrier to internal motion [83]. The barriers between the two stable structures were calculated to be between 6 - 7 kcal/mol and the transition states are

shown in Figure 3.11. An energy diagram of N-methylhydroxylamine is shown in Figure 3.12.

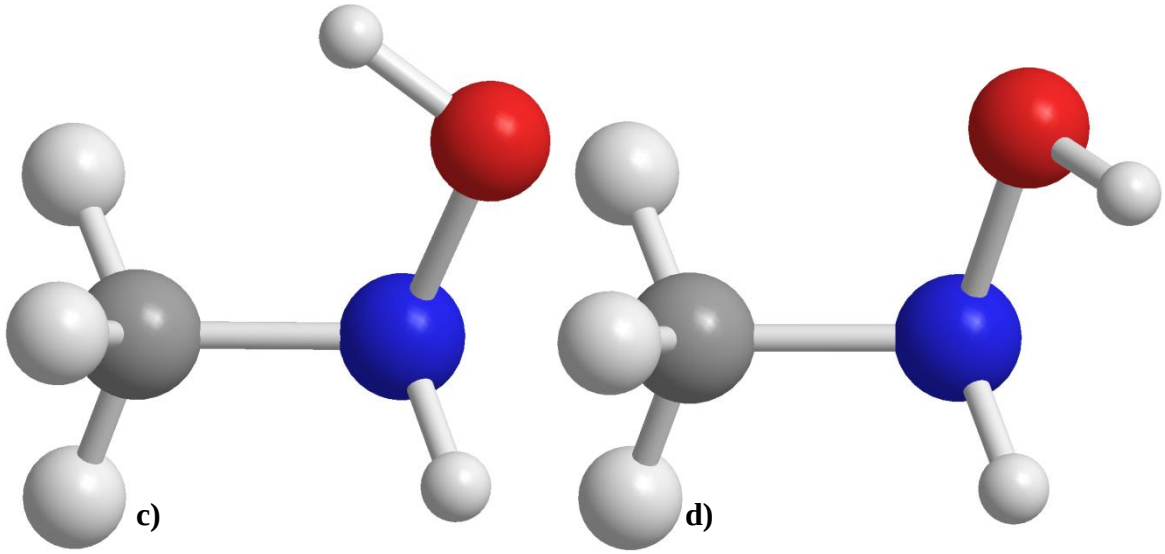

Figure 3.11. Transition states of N-methylhydroxylamine at the following relative energies: c) 6.36 kcal/mol; d) 6.95 kcal/mol.

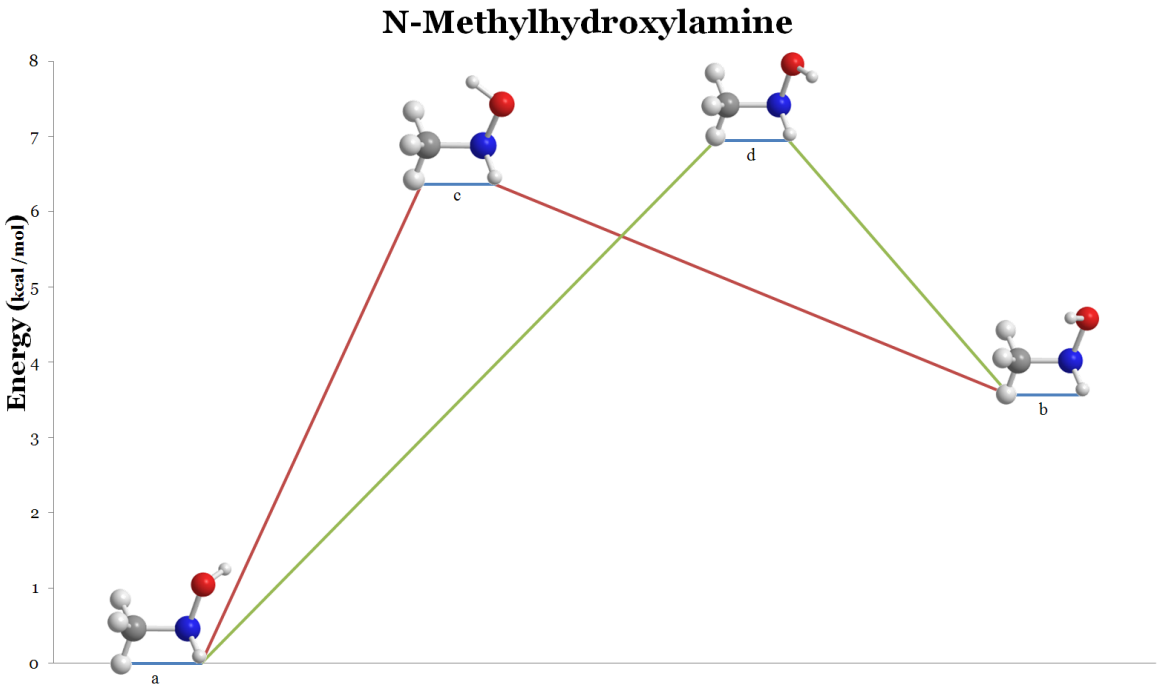

Figure 3.12. Relative energies of the stationary points for N-methylhydroxylamine. Labels correspond to the geometries shown in Figures 3.10 and 3.11.

Further structural information on the stable and transition states of N-methylhydroxylamine can be found in Appendix B.

Chapter 4

Triplet State Product Optimizations

4.1 Introduction

In order to have a better understanding of the possible energy distribution of the target molecules, the triplet states of methanediol, methoxymethanol, aminomethanol, and N-methylhydroxylamine were also probed. All sources of $O(^1D)$ have a probability of forming $O(^3P)$. Because it is in a high energy state, $O(^1D)$ can relax into the ground state from collisions. With the high possibility of producing ground state atomic oxygen, there is a high possibility of producing triplet state molecules because a reaction between triplet atomic oxygen and the singlet ground states of the starting materials, methanol, dimethyl ether, and aminomethanol, would produce a triplet state molecule [27 - 29]. A thorough search of the literature finds no theoretical or experimental data on the triplet structures of the target molecules for comparison.

The optimizations of the triplet states were performed at the Møller-Plesset, MP2 level of perturbation theory [68, 69] with the augmented Dunning correlation consistent triple zeta basis set, Aug-cc-pVTZ [70, 71], using the Gaussian 09 software package [72]. The initial structure input for each molecule was determined using the ACD/ChemSketch software [74]. The geometry optimization function within this program uses a molecular mechanics force field, modified from CHARMM parameterization [73]. The geometries were then used as the input to Gaussian, and individually optimized at increasing levels

of theory up to the MP2/Aug-cc-pVTZ level. The specific calculation details and the results of these optimizations are given below for each molecule.

4.2 Methanediol

In the same way in which the singlet conformers were optimized, the two hydroxyl groups of methanediol were rotated in 90° increments for the initial triplet structures. The optimization calculations on each geometry were performed in the following order: B3LYP/6-311+G**, B3LYP/6-311++G(2d,p), MP2/6-311+G(2d,p), MP2/6-311+G(2df,pd), MP2/cc-pVTZ, and MP2/Aug-cc-pVTZ. Only one structure optimization did not fail when the MP2 optimization was attempted, and this structure is shown in Figure 4.01 a). Six of the seven structures failed to converge when MP2 optimization was attempted on the DFT optimized structures regardless of basis set. The lack of a minimum structure implies that the molecule has no stable triplet structure and any triplet oxygen will react with methanol and fragment the molecule. The optimizations continued for the optimized structures found using the B3LYP level of theory with the following basis sets: 6-311++G(df,pd), 6-311++G(df,2pd), 6-311++G(2df,pd), 6-311++G(2df,2pd), 6-311++G(2df,3pd), cc-pVTZ, 6-311++G(3df,2pd), 6-311++G(3df,3pd), 6-311++G(3df,3p2d), 6-311++G(3d2f,3pd), 6-311++G(3d2f,3p2d). These structures converged to structures similar to Figure 4.01 b) with a single H extended past 2.0Å indicating dissociation.

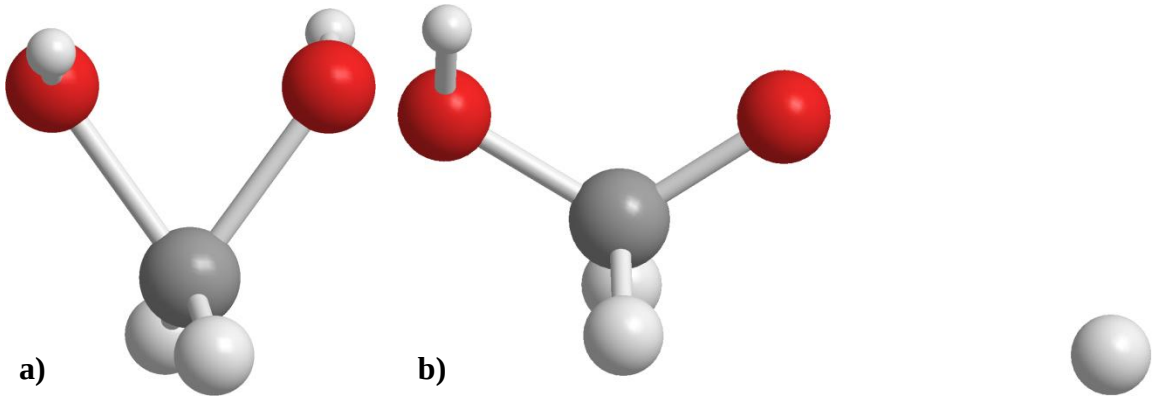

Figure 4.01. Triplet structures of methanediol: a) 163.04 kcal/mol transition structure relative to singlet methanediol; b) H dissociation structure.

The a) structure is shown to be similar to the a) singlet structure aside from differences in the C-O bond lengths. A frequency calculation at MP2/Aug-cc-pVTZ level on the a) triplet structure showed it to not be a stable structure but a transition state due to a single negative frequency. An energy diagram of singlet and triplet methanediol is shown in Figure 4.02.

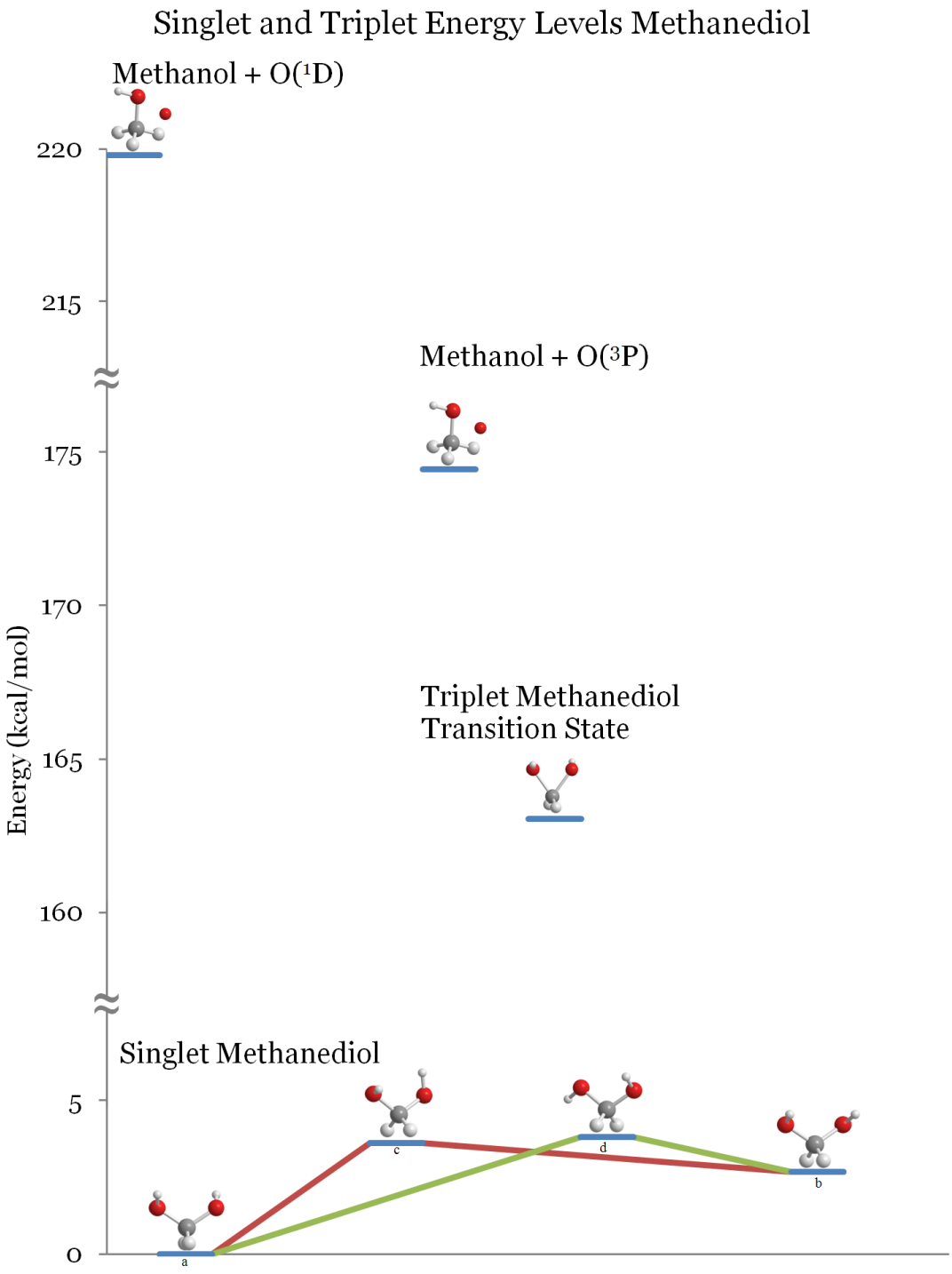

Figure 4.02. Relative energy level diagram of the singlet and triplet states of methanediol.

Further structural information on the stable triplet state of methanediol can be found in Appendix C.

4.3 Methoxymethanol

In the same way in which the singlet conformers were probed, 24 initial geometries of methoxymethanol were obtained by rotating the methyl and hydroxyl groups in 45° increments. None of the triplet geometries converged using an MP2 level of theory, and so the conformers were optimized with B3LYP theory with the following basis sets: 6-311+G, 6-311++G, 6-311++G*, 6-311++G**, 6-311++G(2df,2pd), cc-pVTZ, 6-311++G(3df,3p2d), 6-311++G(3d2f,3p2d), Aug-cc-pVTZ. All 24 geometries resulted in dissociation structures with the hydroxyl proton extended past 2.5Å. An example structure is shown in Figure 4.03 and an overall energy diagram of the states of methoxymethanol and the starting materials are shown in Figure 4.04.

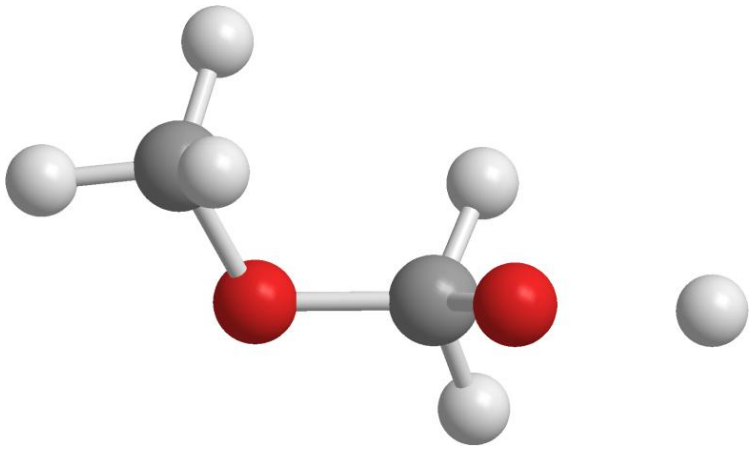

Figure 4.03. Example triplet dissociation structure of methoxymethanol.

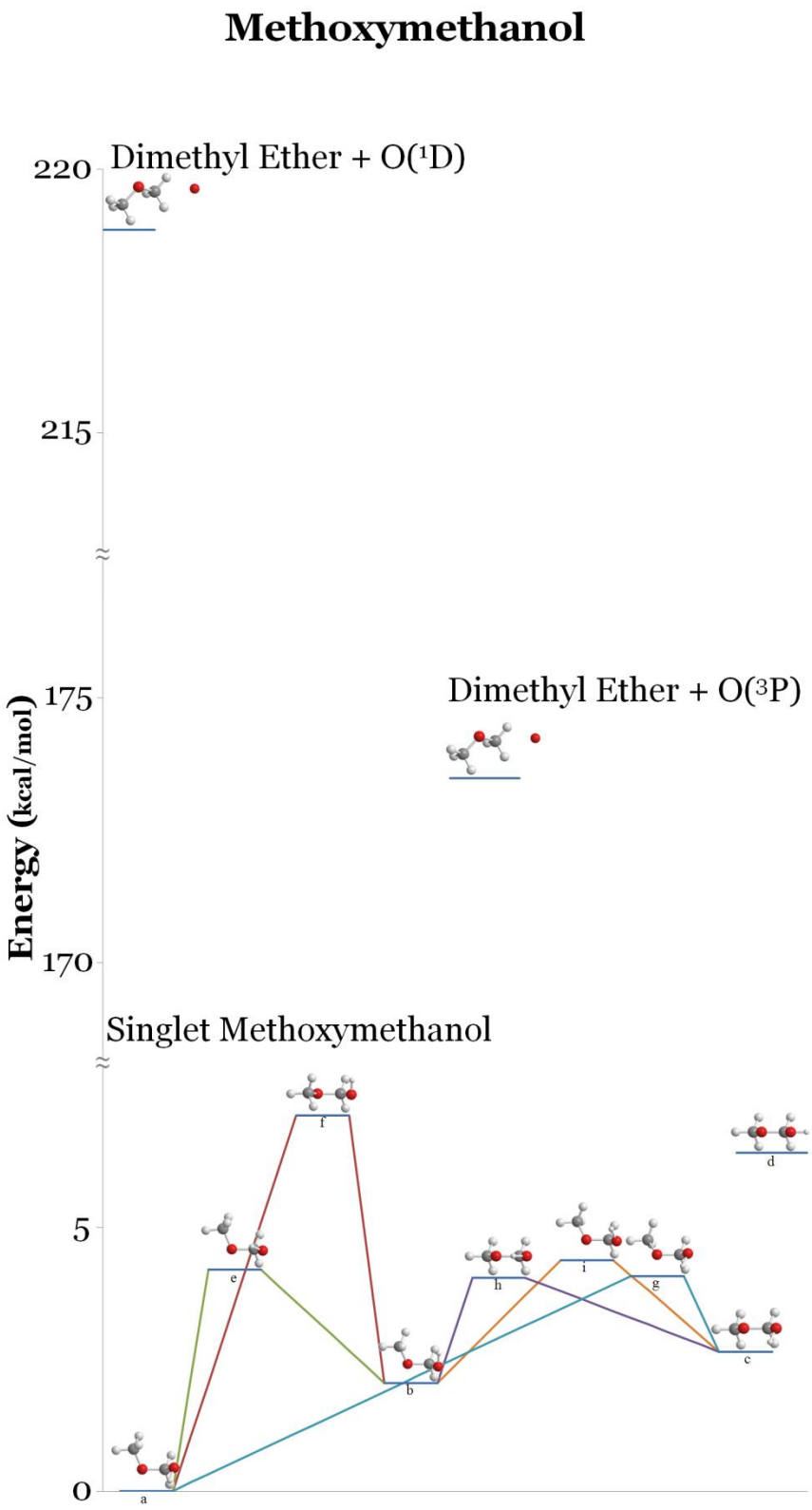

Figure 4.04. Relative energy levels of the singlet and triplet states of methoxymethanol and the starting reactants, dimethyl ether, O(^{3}P), and O(^{1}D).

4.4 Aminomethanol

In the same way in which the singlet conformers were probed, ten initial geometries were obtained by rotating the hydroxyl group and the amine hydrogens in 90° increments. The geometries were optimized at the following levels: B3LYP/6-311++G**, MP2/6-311++G(df,pd), MP2/6-311++G(2df,2pd), MP2/6-311++G(3df,3pd), MP2/6-311++G(3d2f,3p2d), and MP2/Aug-cc-pVTZ. The optimizations converged to two stable structures and several dissociation structures with the hydroxyl or amine protons extended past 2.5 Å. A transition between the two stable states was found using the QST2 function. The spectral parameters of the two stable conformers are shown in Table 4.01 and the stable structures are shown in Figure 4.05 a) and b), the transition structure is shown in Figure 4.05 c), and example dissociation structures are shown in Figure 4.05 d) and e).

Table 4.01. Spectral parameters for the two triplet conformers of aminomethanol calculated using MP2 perturbation theory and Aug-cc-pVTZ basis set.

Parameter	Conformer a	Conformer b
Energy	0 kcal/mol	1.55 kcal/mol
Energy Relative to Singlet Aminomethanol	132.31 kcal/mol	133.81 kcal/mol
A	41.7443976 GHz	40.7846665 GHz
B	10.0083026 GHz	9.6929910 GHz
C	8.5014276 GHz	8.4239094 GHz
μ_x	-6.7313 D	-4.7221 D
μ_y	0.2223 D	0.9481 D
μ_z	0.0036 D	0.4864 D

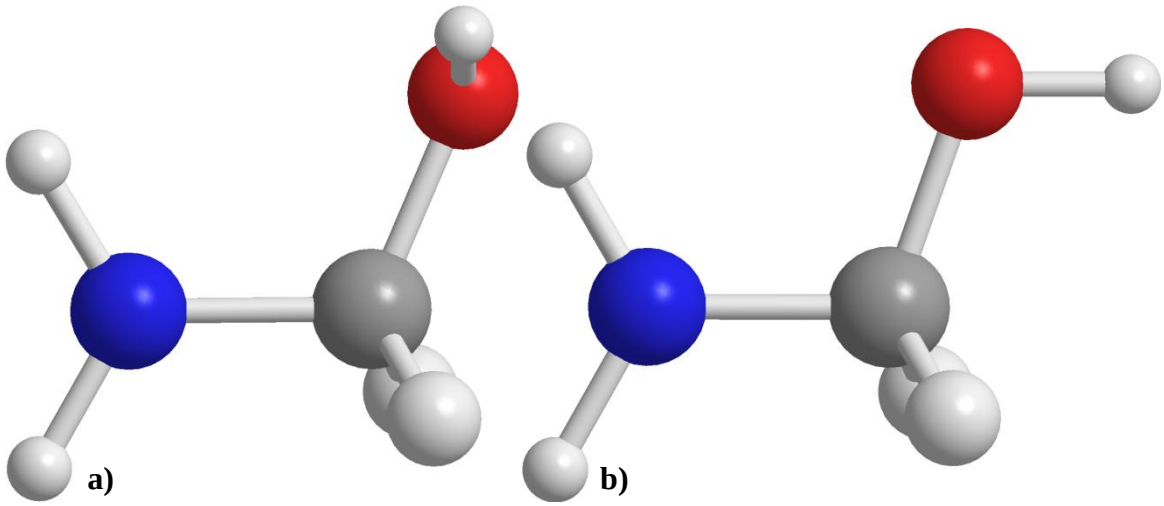

a) **b)**

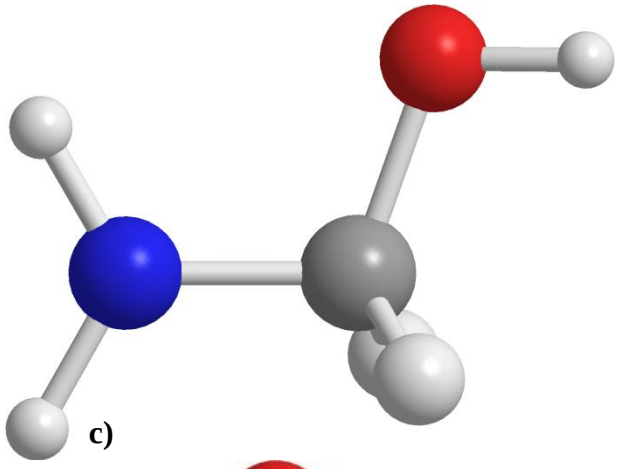

c)

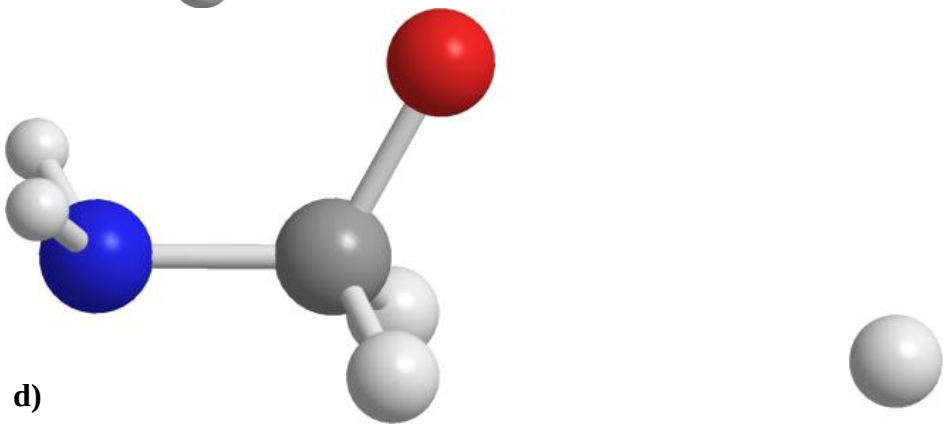

d)

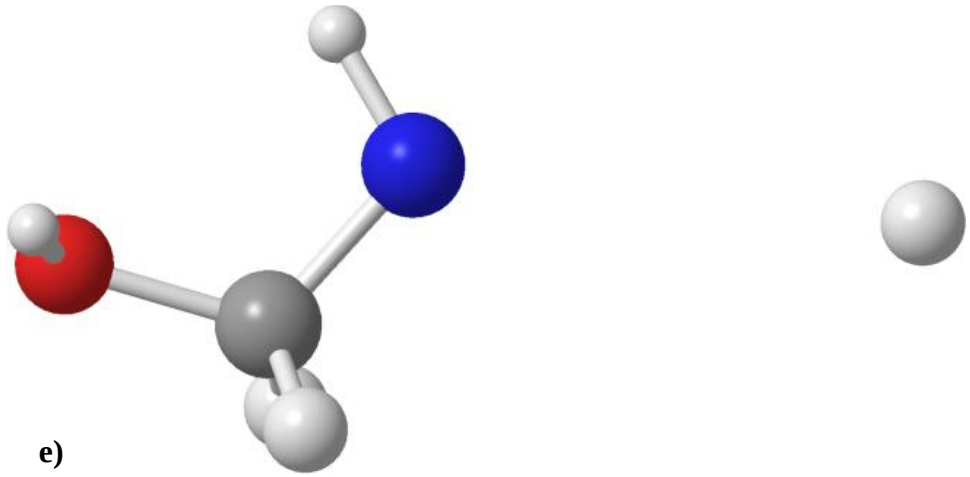

e)

Figure 4.05. Triplet structures of aminomethanol optimized at MP2/Aug-cc-pVTZ theory level: a) ground state triplet conformer; b) higher energy conformer; c) 1.56 kcal/mol barrier between the a and b conformers; d) hydroxyl H dissociation ; e) amine H dissociation.

The amine group of the stable triplet structures is shown to have a trigonal planar geometry as opposed to the pyramidal orientation of the singlet structures. An energy diagram of the triplet stable and transition states is shown in Figure 4.06.

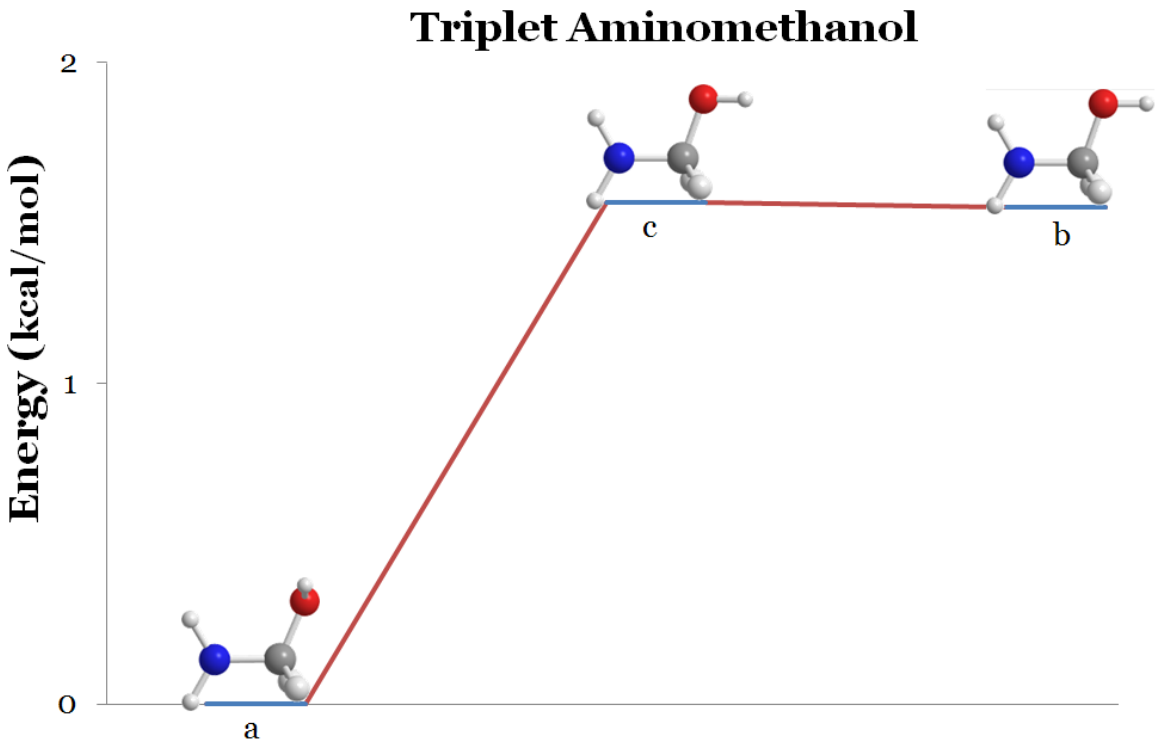

Figure 4.06. Relative energy level diagram of triplet aminomethanol.

Further structural information on the stable triplet states of aminomethanol can be found in Appendix C.

4.5 N-Methylhydroxylamine

In the same way in which the singlet conformers were probed, the triplet conformations of N-methylhydroxylamine were probed using four initial geometries obtained by rotating the hydroxyl group by 90° increments. The geometries were optimized at the following levels: B3LYP/6-311+G(2d,p), B3LYP/6-311++G(2d,p), B3LYP/6-311++G(2df,pd), MP2/6-311++G(2df,pd), MP2/6-311++G(2df,2pd), MP2/6-311++G(2df,3pd), MP2/6-311++G(3df,2pd), MP2/6-311++G(3d2f,3pd), MP2/6-311++G(3d2f,3p2d), MP2/cc-pVTZ, MP2/Aug-cc-pVTZ. All of the initial geometries

converge to an OH dissociation structure in which the OH fragment is about 2Å from the nitrogen, as shown in Figure 4.07.

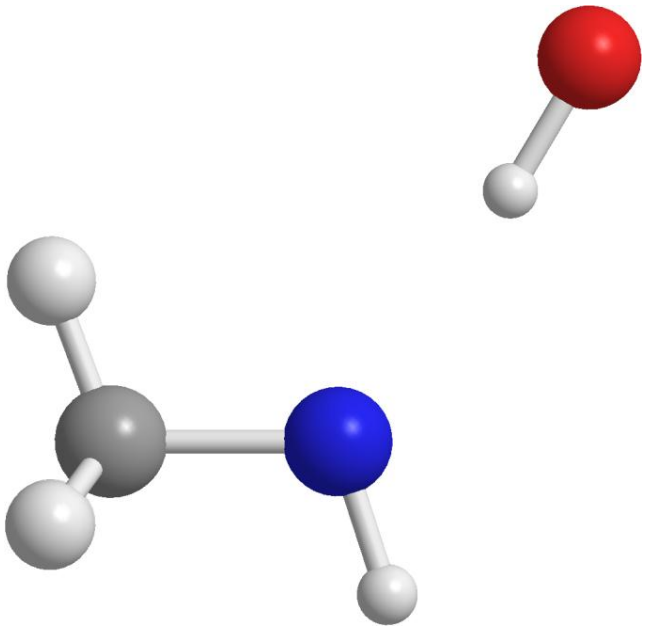

Figure 4.07. Triplet dissociation structure of N-methylhydroxylamine.

The overall energy diagram of the singlet and triplet states of aminomethanol, N-methylhydroxylamine, and their starting materials is shown in Figure 4.08.

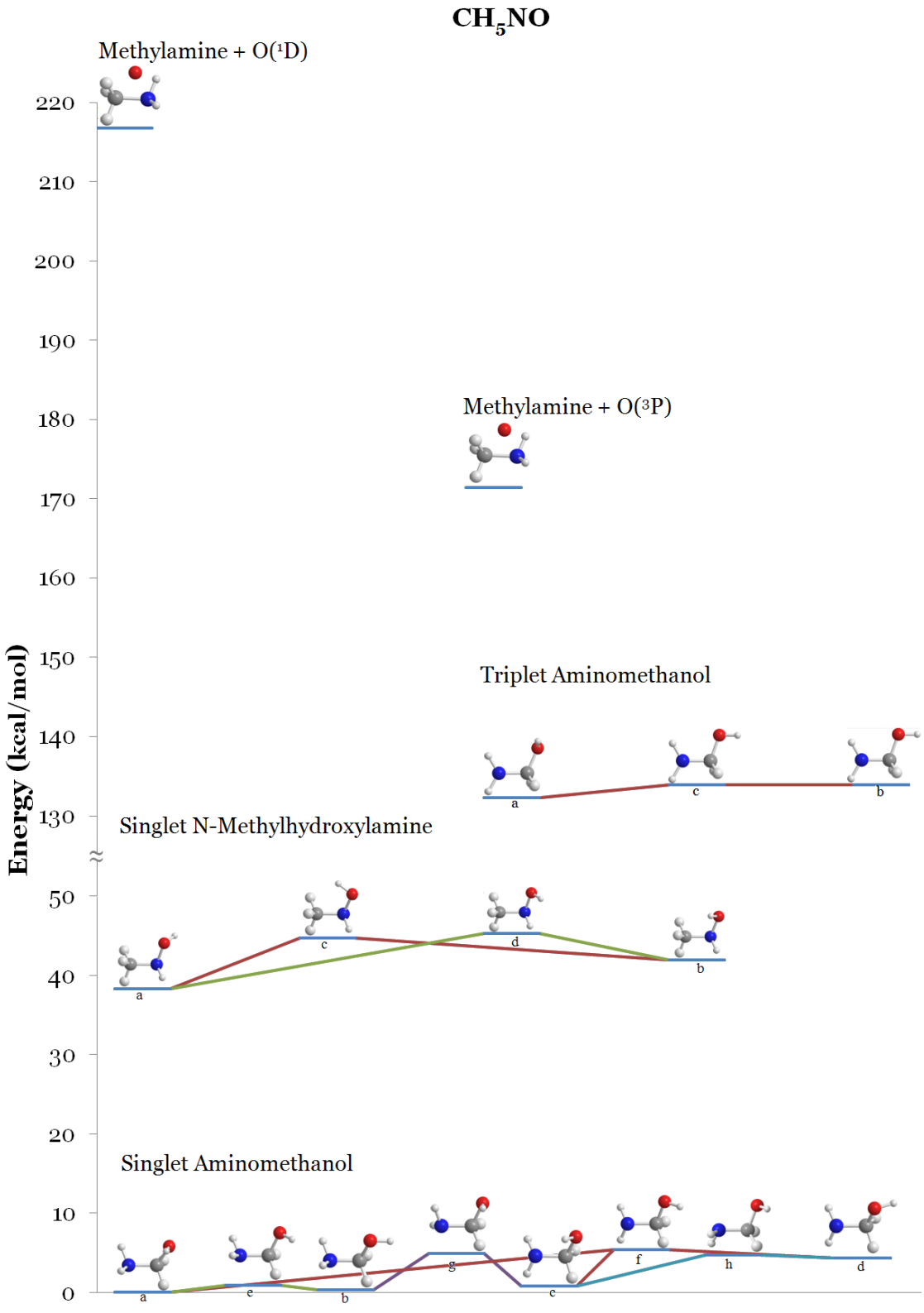

Figure 4.08. Relative energy levels of the singlet and triplet states of aminomethanol, singlet N-methylhydroxylamine, and the starting reactants, methylamine, $O(^3P)$, and $O(^1D)$.

Figure 4.08 shows a greater energy difference O(^{1}D) and aminomethanol, but the starting material for the triplet state is much lower in energy and closer in energy to the final triplet product.

Chapter 5

Discussion and Conclusions

5.1 Introduction

The calculations presented here were used to determine the likelihood of formation of the target molecules methanediol, methoxymethanol, and aminomethanol from $O(^1D)$ reactions. In each case, the formation from $O(^1D)$ is shown to be highly exothermic, and the singlet states of the molecules are energetically favored.

Beyond the reaction energetics, the calculations shown here can be used to investigate the anticipated spectral complexity. This complexity might arise from spectral interference from triplet state products as well as from internal motion of the methyl groups and hydroxyl groups. A stable triplet state might compete with the production pathway of the singlet state, reducing the total yield of the singlet state and weakening its spectrum, and also adding spectral complexity from the triplet state. However, only one local energy minimum was found on a triplet surface for the target molecules. It is therefore unlikely that triplet states will contribute greatly to the observed spectra of these species.

Given the lack of interference from triplet states, internal motion contributions will dominate the spectral complexity. The results of the calculations presented here can be used to determine some of the barriers to internal motion. These barriers can then be used to predict the spectral line splitting in the pure rotational spectrum. In microwave spectroscopy, the primary tool for predicting and assigning spectra is the CALPGM software

suite [84]. SPCAT uses spectroscopic parameters, dipole moments, and partition functions from calculations to generate spectral predictions. A root-mean-squared fitting routine, SPFIT, that uses a user-defined Hamiltonian with the assigned spectral data can then be used to further refine these parameters. This program has recently been upgraded to incorporate internal rotation Hamiltonians [85].

The implications for each molecule, including the relative energies of the stationary points on the potential energy surface, the insertion reaction energetics, the expected contributions from the triplet states, and the expected internal motion contribution to spectral complexity, are summarized below.

5.2 Methanediol

Figure 4.02 shows the relative energies of the singlet and triplet states and the starting materials. The formation of singlet methanediol is more energetically favored than the triplet state. The formation of the singlet product releases 219.8 kcal/mol of energy, whereas the formation of the triplet product releases only 11.4 kcal/mol.

The only triplet stationary point found for methanediol is a transition state. Since all other stationary points found from the triplet calculations are dissociated structures, the transition state should lead to those fragmented forms of methanediol. This reaction pathway is unlikely in a supersonic expansion, where the rotational and vibrational cooling will likely favor product formation in the singlet state.

The barriers between the two stable states of methanediol are about 1300 cm^{-1} which indicates hindered wagging motion of the hydroxyl groups. While some rotational

spectral line splitting may occur, this splitting should be quite small, and the resultant spectrum should be straightforward to assign.

5.3 Methoxymethanol

The relative energies of methoxymethanol can be seen in Figure 4.04. The singlet structure of methoxymethanol is highly favored due to a 218.8 kcal/mol release of energy. The triplet calculations yield no possible stable structures aside from dissociations and therefore simplify the possible distribution of products in laboratory spectral acquisitions.

The barriers to rotation of the methoxy and hydroxyl groups from the minimum energy state of methoxymethanol are in the range of 1428 – 2495 cm^{-1}, which are extremely high and this molecule is therefore expected to be nearly-rigid. Lacking from this study were calculations on the methyl rotations, the barrier of which is expected to be low and cause spectral splittings.

5.4 Aminomethanol and N-Methylhydroxylamine

The relative energies of aminomethanol and N-methylhydroxylamine can be seen in Figure 4.08. The singlet structure of aminomethanol is energetically favored over singlet N-methylhydroxylamine and triplet state aminomethanol. The production of triplet aminomethanol yields only 39.1 kcal/mol of energy. There are 216.8 kcal/mol of energy released upon formation of the lowest energy singlet conformation of aminomethanol. The exothermic energy released from producing singlet N-methylhydroxylamine is 38.4 kcal/mol less than that of aminomethanol.

The search for triplet N-methylhydroxylamine yielded only dissociation structures but two stable structures are found for triplet aminomethanol. Triplet aminomethanol is much less favored than the singlet state because the lowest energy conformer of triplet aminomethanol is higher in energy than the singlet by 132.3 kcal/mol. In spite of the low favorability of the triplet state, the existence of stable triplet structures complicates possible laboratory spectra.

Another possible complication to the aminomethanol spectra is internal motion. All but one barrier of aminomethanol are within the 1380 – 1875 cm^{-1} range and result in very hindered motions. The e) barrier is 325 cm^{-1} and indicate reasonably unhindered hydroxyl wagging. This internal motion will complicate the rotational spectrum of aminomethanol.

5.5 Summary

The calculations show the most energetically-favored products resulting from the reactions of atomic oxygen with methanol, dimethyl ether, and methylamine are the singlet states of methanediol, methoxymethanol, and aminomethanol, respectively. Each of these insertion reactions is predicted to be highly exothermic. Only the triplet state of aminomethanol has stable energy minima, and this triplet surface is considerably higher in energy than the singlet surface. The target species in their singlet states will therefore be the most favored and likely insertion reaction products, greatly simplifying the possible distribution of products in the laboratory studies.

Despite the experimental simplification concerning triplet reaction products, the laboratory spectral acquisition for these species will not be straightforward. The most severe complication will be from the intricate spectral patterns arising from complex internal motion for each of the target molecules. While the assignment of spectral lines is more straightforward for molecules with little internal motion, spectral line splitting arising from internal motion is often quite helpful in identification of molecules in astronomical spectra, as it provide a distinct spectral fingerprint for the molecule. The fluxional barriers for methanediol are in the range of 1262-2494 cm^{-1}, and so spectral complication should be minimal for this molecule. Methoxymethanol will likely have splitting due to rotations of the methyl group, but the barrier for this motion has not been calculated in this study. Aminomethanol, however, is expected to have a 325 cm^{-1} barrier to wagging of the hydroxyl group. This low barrier will extremely complicate the spectrum for this molecule.

Further investigation of the potential energy surfaces of methanediol, methoxymethanol, and aminomethanol are needed to fully characterize the singlet and triplet surfaces and find surface crossings. The work presented here provides an excellent starting point for more advanced methods of calculation to complete the surfaces and also gives the structural information needed to predict and assign the rotational spectra of these molecules.

Appendix A

Starting Materials

Table A.01. Methanol geometry optimized at the MP2/Aug-cc-pVTZ theory level.

Atom 1	Atom 2	Bond Length (Angstroms)	Atom 3	Angle (degrees)	Atom 4	Torsion Angle (degrees)
C(1)						
O(2)	C(1)	1.4233				
H(3)	C(1)	1.0913	O(2)	111.9352		
H(4)	C(1)	1.0859	O(2)	106.4966	H(3)	108.5786
H(5)	C(1)	1.0913	O(2)	111.9352	H(3)	109.1817
H(6)	O(2)	0.9611	C(1)	108.0089	H(3)	61.4792

Table A.02. Dimethyl ether geometry optimized at the MP2/Aug-cc-pVTZ theory level.

Atom 1	Atom 2	Bond Length (Angstroms)	Atom 3	Angle (degrees)	Atom 4	Torsion Angle (degrees)
C(1)						
O(2)	C(1)	1.4116				
C(3)	O(2)	1.4116	C(1)	110.6626		
H(4)	C(1)	1.0952	O(2)	111.1468	C(3)	60.5335
H(5)	C(1)	1.0864	O(2)	107.4242	H(4)	109.2511
H(6)	C(1)	1.0952	O(2)	111.1468	H(4)	108.5863
H(7)	C(3)	1.0952	O(2)	111.1468	C(1)	-60.5335
H(8)	C(3)	1.0952	O(2)	111.1468	H(7)	108.5863
H(9)	C(3)	1.0864	O(2)	107.4242	H(7)	109.2511

Table A.03. Methylamine geometry optimized at the MP2/Aug-cc-pVTZ theory level.

Atom 1	Atom 2	Bond Length (Angstroms)	Atom 3	Angle (degrees)	Atom 4	Torsion Angle (degrees)
C(1)						
N(2)	C(1)	1.4643				
H(3)	C(1)	1.0938	N(2)	114.8866		
H(4)	C(1)	1.0881	N(2)	108.9773	H(3)	108.1714
H(5)	C(1)	1.0881	N(2)	108.9773	H(3)	108.1714
H(6)	N(2)	1.0121	C(1)	110.2469	H(3)	-58.5081
H(7)	N(2)	1.0121	C(1)	110.2469	H(6)	106.2650

Appendix B

Singlet Molecules

B.1 Singlet Methanediol

Table B.01. Methanediol a) structure optimized at the MP2/Aug-cc-pVTZ theory level.

Atom 1	Atom 2	Bond Length (Angstroms)	Atom 3	Angle (degrees)	Atom 4	Torsion Angle (degrees)
C(1)						
O(2)	C(1)	1.4064				
O(3)	C(1)	1.4064	O(2)	112.7339		
H(4)	C(1)	1.0891	O(2)	111.8605	O(3)	105.1278
H(5)	C(1)	1.0891	O(2)	105.1278	O(3)	111.8605
H(6)	O(2)	0.9640	C(1)	107.4118	O(3)	-61.7300
H(7)	O(3)	0.9640	C(1)	107.4118	O(2)	-61.7300

Table B.02. Methanediol b) structure optimized at the MP2/Aug-cc-pVTZ theory level.

Atom 1	Atom 2	Bond Length (Angstroms)	Atom 3	Angle (degrees)	Atom 4	Torsion Angle (degrees)
C(1)						
O(2)	C(1)	1.4071				
O(3)	C(1)	1.4071	O(2)	113.7625		
H(4)	C(1)	1.0931	O(2)	110.4894	O(3)	110.4894
H(5)	C(1)	1.0845	O(2)	105.8534	O(3)	105.8534
H(6)	O(2)	0.9623	C(1)	108.9307	O(3)	-78.7877
H(7)	O(3)	0.9623	C(1)	108.9308	O(2)	78.7866

Table B.03. Methanediol c) structure optimized at the MP2/Aug-cc-pVTZ theory level.

Atom 1	Atom 2	Bond Length (Angstroms)	Atom 3	Angle (degrees)	Atom 4	Torsion Angle (degrees)
C(1)						
O(2)	C(1)	1.4074				
O(3)	C(1)	1.4134	O(2)	111.9645		
H(4)	C(1)	1.0923	O(2)	110.4921	O(3)	109.6133
H(5)	C(1)	1.0869	O(2)	107.3373	O(3)	107.3070
H(6)	O(2)	0.9618	C(1)	108.5231	O(3)	-94.3959
H(7)	O(3)	0.9630	C(1)	106.5525	O(2)	18.1128

Table B.04. Methanediol d) structure optimized at the MP2/Aug-cc-pVTZ theory level.

Atom 1	Atom 2	Bond Length (Angstroms)	Atom 3	Angle (degrees)	Atom 4	Torsion Angle (degrees)
C(1)						
O(2)	C(1)	1.4186				
O(3)	C(1)	1.3934	O(2)	108.9752		
H(4)	C(1)	1.0939	O(2)	109.3880	O(3)	110.9567
H(5)	C(1)	1.0891	O(2)	111.2304	O(3)	106.1424
H(6)	O(2)	0.9622	C(1)	108.8677	O(3)	152.9328
H(7)	O(3)	0.9635	C(1)	107.6830	O(2)	61.9556

B.2 Singlet Methoxymethanol

Table B.05. Methoxymethanol a) structure optimized at the MP2/Aug-cc-pVTZ theory level.

Atom 1	Atom 2	Bond Length (Angstroms)	Atom 3	Angle (degrees)	Atom 4	Torsion Angle (degrees)
C(1)						
O(2)	C(1)	1.3987				
O(3)	C(1)	1.4093	O(2)	113.2539		
C(4)	O(2)	1.4227	C(1)	112.1259	O(3)	67.4601
H(5)	C(1)	1.0895	O(2)	105.4929	O(3)	111.5562
H(6)	C(1)	1.0926	O(2)	110.9070	O(3)	105.0630
H(7)	C(4)	1.0856	O(2)	106.7896	C(1)	178.0600
H(8)	C(4)	1.0897	O(2)	111.2776	H(7)	109.7701
H(9)	C(4)	1.0936	O(2)	110.3973	H(7)	109.4427
H(10)	O(3)	0.9639	C(1)	107.3142	O(2)	64.7062

Table B.06. Methoxymethanol b) structure optimized at the MP2/Aug-cc-pVTZ theory level.

Atom 1	Atom 2	Bond Length (Angstroms)	Atom 3	Angle (degrees)	Atom 4	Torsion Angle (degrees)
C(1)						
O(2)	C(1)	1.3991				
O(3)	C(1)	1.4096	O(2)	113.8349		
C(4)	O(2)	1.4162	C(1)	112.4437	O(3)	68.6550
H(5)	C(1)	1.0851	O(2)	105.8687	O(3)	106.5735
H(6)	C(1)	1.0971	O(2)	109.6154	O(3)	110.1094
H(7)	C(4)	1.0857	O(2)	107.1083	C(1)	171.8517
H(8)	C(4)	1.0920	O(2)	111.4905	H(7)	108.8648
H(9)	C(4)	1.0956	O(2)	110.8058	H(7)	109.1564
H(10)	O(3)	0.9617	C(1)	108.9034	O(2)	-86.5656

Table B.07. Methoxymethanol c) structure optimized at the MP2/Aug-cc-pVTZ theory level.

Atom 1	Atom 2	Bond Length (Angstroms)	Atom 3	Angle (degrees)	Atom 4	Torsion Angle (degrees)
C(1)						
O(2)	C(1)	1.4099				
O(3)	C(1)	1.3900	O(2)	109.2425		
C(4)	O(2)	1.4161	C(1)	110.6999	O(3)	-178.5491
H(5)	C(1)	1.0992	O(2)	108.8689	O(3)	111.9944
H(6)	C(1)	1.0932	O(2)	110.6120	O(3)	106.5353
H(7)	C(4)	1.0855	O(2)	107.1023	C(1)	179.4387
H(8)	C(4)	1.0941	O(2)	111.1666	H(7)	109.1987
H(9)	C(4)	1.0945	O(2)	111.2790	H(7)	109.2797
H(10)	O(3)	0.9637	C(1)	107.4637	O(2)	59.3301

Table B.08. Methoxymethanol d) structure optimized at the MP2/Aug-cc-pVTZ theory level.

Atom 1	Atom 2	Bond Length (Angstroms)	Atom 3	Angle (degrees)	Atom 4	Torsion Angle (degrees)
C(1)						
O(2)	C(1)	1.3944				
O(3)	C(1)	1.4026	O(2)	104.9473		
C(4)	O(2)	1.4150	C(1)	110.5675	O(3)	-179.8595
H(5)	C(1)	1.1001	O(2)	109.9682	O(3)	111.2989
H(6)	C(1)	1.1001	O(2)	109.9824	O(3)	111.2987
H(7)	C(4)	1.0853	O(2)	106.9294	C(1)	-179.9989
H(8)	C(4)	1.0945	O(2)	111.2574	H(7)	109.2562
H(9)	C(4)	1.0945	O(2)	111.2559	H(7)	109.2593
H(10)	O(3)	0.9628	C(1)	107.9751	O(2)	-179.4715

Table B.09. Methoxymethanol e) structure optimized at the MP2/Aug-cc-pVTZ theory level.

Atom 1	Atom 2	Bond Length (Angstroms)	Atom 3	Angle (degrees)	Atom 4	Torsion Angle (degrees)
C(1)						
O(2)	C(1)	1.3976				
O(3)	C(1)	1.4176	O(2)	113.0960		
C(4)	O(2)	1.4213	C(1)	112.8560	O(3)	82.2897
H(5)	C(1)	1.0872	O(2)	106.9834	O(3)	107.2635
H(6)	C(1)	1.0960	O(2)	109.8594	O(3)	109.1961
H(7)	C(4)	1.0856	O(2)	106.8400	C(1)	177.5512
H(8)	C(4)	1.0933	O(2)	112.1474	H(7)	108.7840
H(9)	C(4)	1.0925	O(2)	110.6701	H(7)	109.5541
H(10)	O(3)	0.9625	C(1)	107.3799	O(2)	-18.5649

Table B.10. Methoxymethanol f) structure optimized at the MP2/Aug-cc-pVTZ theory level.

Atom 1	Atom 2	Bond Length (Angstroms)	Atom 3	Angle (degrees)	Atom 4	Torsion Angle (degrees)
C(1)						
O(2)	C(1)	1.4221				
O(3)	C(1)	1.4021	O(2)	114.9731		
C(4)	O(2)	1.4180	C(1)	116.8217	O(3)	4.6835
H(5)	C(1)	1.0882	O(2)	107.4390	O(3)	106.1007
H(6)	C(1)	1.0927	O(2)	107.3262	O(3)	110.8597
H(7)	C(4)	1.0862	O(2)	105.3377	C(1)	-177.6866
H(8)	C(4)	1.0893	O(2)	112.2431	H(7)	109.5146
H(9)	C(4)	1.0932	O(2)	112.3185	H(7)	108.4840
H(10)	O(3)	0.9619	C(1)	108.7447	O(2)	-82.4849

Table B.11. Methoxymethanol g) structure optimized at the MP2/Aug-cc-pVTZ theory level.

Atom 1	Atom 2	Bond Length (Angstroms)	Atom 3	Angle (degrees)	Atom 4	Torsion Angle (degrees)
C(1)						
O(2)	C(1)	1.4098				
O(3)	C(1)	1.3985	O(2)	110.5918		
C(4)	O(2)	1.4174	C(1)	113.3695	O(3)	132.5855
H(5)	C(1)	1.0944	O(2)	108.5696	O(3)	110.9633
H(6)	C(1)	1.0910	O(2)	110.6993	O(3)	105.9874
H(7)	C(4)	1.0860	O(2)	106.9318	C(1)	-177.6722
H(8)	C(4)	1.0931	O(2)	110.9069	H(7)	109.3167
H(9)	C(4)	1.0933	O(2)	111.6354	H(7)	108.8705
H(10)	O(3)	0.9635	C(1)	107.5420	O(2)	60.4626

Table B.12. Methoxymethanol h) structure optimized at the MP2/Aug-cc-pVTZ theory level.

Atom 1	Atom 2	Bond Length (Angstroms)	Atom 3	Angle (degrees)	Atom 4	Torsion Angle (degrees)
C(1)						
O(2)	C(1)	1.4064				
O(3)	C(1)	1.3993	O(2)	108.0793		
C(4)	O(2)	1.4170	C(1)	111.3080	O(3)	-179.9734
H(5)	C(1)	1.0969	O(2)	109.9775	O(3)	109.6179
H(6)	C(1)	1.0969	O(2)	109.9800	O(3)	109.6177
H(7)	C(4)	1.0853	O(2)	107.0544	C(1)	179.9880
H(8)	C(4)	1.0935	O(2)	111.0123	H(7)	109.3566
H(9)	C(4)	1.0935	O(2)	111.0111	H(7)	109.3611
H(10)	O(3)	0.9643	C(1)	105.9048	O(2)	0.0022

Table B.13. Methoxymethanol i) structure optimized at the MP2/Aug-cc-pVTZ theory level.

Atom 1	Atom 2	Bond Length (Angstroms)	Atom 3	Angle (degrees)	Atom 4	Torsion Angle (degrees)
C(1)						
O(2)	C(1)	1.4090				
O(3)	C(1)	1.4012	O(2)	111.3024		
C(4)	O(2)	1.4188	C(1)	113.7439	O(3)	122.7363
H(5)	C(1)	1.0883	O(2)	109.3946	O(3)	105.3180
H(6)	C(1)	1.0959	O(2)	109.3198	O(3)	111.3393
H(7)	C(4)	1.0861	O(2)	106.8010	C(1)	-174.9056
H(8)	C(4)	1.0938	O(2)	111.4247	H(7)	109.0789
H(9)	C(4)	1.0925	O(2)	111.5899	H(7)	108.9663
H(10)	O(3)	0.9637	C(1)	107.7703	O(2)	-58.3779

B.3 Singlet Aminomethanol

Table B.14. Aminomethanol a) structure optimized at the MP2/Aug-cc-pVTZ theory level.

Atom 1	Atom 2	Bond Length (Angstroms)	Atom 3	Angle (degrees)	Atom 4	Torsion Angle (degrees)
N(1)						
C(2)	N(1)	1.4375				
O(3)	C(2)	1.4225	N(1)	106.6916		
H(4)	N(1)	1.0109	C(2)	111.6253	O(3)	78.131
H(5)	N(1)	1.0102	C(2)	111.3719	H(4)	108.781
H(6)	C(2)	1.0926	N(1)	107.7592	O(3)	110.8356
H(7)	C(2)	1.0971	N(1)	114.1456	O(3)	108.8359
H(8)	O(3)	0.9629	C(2)	107.7961	N(1)	-162.0924

Table B.15. Aminomethanol b) structure optimized at the MP2/Aug-cc-pVTZ theory level.

Atom 1	Atom 2	Bond Length (Angstroms)	Atom 3	Angle (degrees)	Atom 4	Torsion Angle (degrees)
N(1)						
C(2)	N(1)	1.4482				
O(3)	C(2)	1.4131	N(1)	110.0226		
H(4)	N(1)	1.0118	C(2)	111.4199	O(3)	78.2676
H(5)	N(1)	1.0114	C(2)	111.5560	H(4)	108.3865
H(6)	C(2)	1.093	N(1)	107.4542	O(3)	111.3574
H(7)	C(2)	1.0912	N(1)	114.6459	O(3)	104.6985
H(8)	O(3)	0.9651	C(2)	105.7572	N(1)	44.2582

Table B.16. Aminomethanol c) structure optimized at the MP2/Aug-cc-pVTZ theory level.

Atom 1	Atom 2	Bond Length (Angstroms)	Atom 3	Angle (degrees)	Atom 4	Torsion Angle (degrees)
N(1)						
C(2)	N(1)	1.4262				
O(3)	C(2)	1.4369	N(1)	110.65		
H(4)	N(1)	1.012	C(2)	110.3004	O(3)	-59.3261
H(5)	N(1)	1.012	C(2)	110.3004	H(4)	107.5421
H(6)	C(2)	1.0911	N(1)	108.7071	O(3)	109.7657
H(7)	C(2)	1.0911	N(1)	108.7071	O(3)	109.7656
H(8)	O(3)	0.9642	C(2)	108.4531	N(1)	180.0000

Table B.17. Aminomethanol d) structure optimized at the MP2/Aug-cc-pVTZ theory level.

Atom 1	Atom 2	Bond Length (Angstroms)	Atom 3	Angle (degrees)	Atom 4	Torsion Angle (degrees)
N(1)						
C(2)	N(1)	1.4355				
O(3)	C(2)	1.4305	N(1)	116.1036		
H(4)	N(1)	1.0115	C(2)	111.8433	O(3)	-67.6085
H(5)	N(1)	1.0119	C(2)	110.7682	H(4)	108.1287
H(6)	C(2)	1.0908	N(1)	108.1846	O(3)	110.2581
H(7)	C(2)	1.0865	N(1)	108.8380	O(3)	104.3084
H(8)	O(3)	0.963	C(2)	108.0326	N(1)	68.9519

Table B.18. Aminomethanol e) structure optimized at the MP2/Aug-cc-pVTZ theory level.

Atom 1	Atom 2	Bond Length (Angstroms)	Atom 3	Angle (degrees)	Atom 4	Torsion Angle (degrees)
N(1)						
C(2)	N(1)	1.4315				
O(3)	C(2)	1.4374	N(1)	113.2722		
H(4)	N(1)	1.0122	C(2)	110.5528	O(3)	-58.2935
H(5)	N(1)	1.0120	C(2)	110.2824	H(4)	107.3532
H(6)	C(2)	1.0897	N(1)	108.8100	O(3)	109.7554
H(7)	C(2)	1.0890	N(1)	108.1062	O(3)	107.8768
H(8)	O(3)	0.9610	C(2)	108.7781	N(1)	126.0190

Table B.19. Aminomethanol f) structure optimized at the MP2/Aug-cc-pVTZ theory level.

Atom 1	Atom 2	Bond Length (Angstroms)	Atom 3	Angle (degrees)	Atom 4	Torsion Angle (degrees)
N(1)						
C(2)	N(1)	1.4481				
O(3)	C(2)	1.4195	N(1)	107.1705		
H(4)	N(1)	1.0136	C(2)	109.5114	O(3)	64.8502
H(5)	N(1)	1.0133	C(2)	109.9402	H(4)	107.0759
H(6)	C(2)	1.0912	N(1)	107.8707	O(3)	111.3600
H(7)	C(2)	1.0961	N(1)	113.6034	O(3)	108.2069
H(8)	O(3)	0.9603	C(2)	108.8218	N(1)	140.4439

Table B.20. Aminomethanol g) structure optimized at the MP2/Aug-cc-pVTZ theory level.

Atom 1	Atom 2	Bond Length (Angstroms)	Atom 3	Angle (degrees)	Atom 4	Torsion Angle (degrees)
N(1)						
C(2)	N(1)	1.4634				
O(3)	C(2)	1.4178	N(1)	111.6210		
H(4)	N(1)	1.0132	C(2)	107.6615	O(3)	6.7267
H(5)	N(1)	1.0118	C(2)	110.7370	H(4)	106.1287
H(6)	C(2)	1.0911	N(1)	109.5019	O(3)	109.6496
H(7)	C(2)	1.0891	N(1)	111.3582	O(3)	106.1048
H(8)	O(3)	0.9622	C(2)	107.8657	N(1)	81.8842

Table B.21. Aminomethanol h) structure optimized at the MP2/Aug-cc-pVTZ theory level.

Atom 1	Atom 2	Bond Length (Angstroms)	Atom 3	Angle(degrees)	Atom 4	Torsion Angle (degrees)
N(1)						
C(2)	N(1)	1.4435				
O(3)	C(2)	1.4210	N(1)	109.5196		
H(4)	N(1)	1.0113	C(2)	111.9929	O(3)	80.2473
H(5)	N(1)	1.0111	C(2)	111.2311	H(4)	108.4894
H(6)	C(2)	1.0898	N(1)	107.4099	O(3)	108.4485
H(7)	C(2)	1.0954	N(1)	114.0572	O(3)	108.8983
H(8)	O(3)	0.9602	C(2)	108.4198	N(1)	-118.5932

B.4 Singlet N-Methylhydroxylamine

Table B.22. N-methylhydroxylamine a) structure optimized at the MP2/Aug-cc-pVTZ theory level.

Atom 1	Atom 2	Bond Length (Angstroms)	Atom 3	Angle (degrees)	Atom 4	Torsion Angle (degrees)
N(1)						
C(2)	N(1)	1.4564				
O(3)	N(1)	1.4457	C(2)	106.4182		
H(4)	N(1)	1.0157	C(2)	107.9347	O(3)	102.5761
H(5)	C(2)	1.0926	N(1)	112.7107	O(3)	-49.7308
H(6)	C(2)	1.0869	N(1)	109.0226	H(5)	109.0706
H(7)	C(2)	1.0898	N(1)	107.5675	H(5)	109.5584
H(8)	O(3)	0.9633	N(1)	102.0626	C(2)	-125.8409

Table B.23. N-methylhydroxylamine b) structure optimized at the MP2/Aug-cc-pVTZ theory level.

Atom 1	Atom 2	Bond Length (Angstroms)	Atom 3	Angle (degrees)	Atom 4	Torsion Angle (degrees)
N(1)						
C(2)	N(1)	1.4521				
O(3)	N(1)	1.4295	C(2)	109.2075		
H(4)	N(1)	1.0163	C(2)	109.4941	O(3)	105.6758
H(5)	C(2)	1.0983	N(1)	113.3318	O(3)	-55.3851
H(6)	C(2)	1.0869	N(1)	108.7402	H(5)	108.8582
H(7)	C(2)	1.0894	N(1)	108.0396	H(5)	108.7765
H(8)	O(3)	0.9707	N(1)	106.5295	C(2)	51.7071

Table B.24. N-methylhydroxylamine c) structure optimized at the MP2/Aug-cc-pVTZ theory level.

Atom 1	Atom 2	Bond Length (Angstroms)	Atom 3	Angle (degrees)	Atom 4	Torsion Angle (degrees)
N(1)						
C(2)	N(1)	1.4548				
O(3)	N(1)	1.4549	C(2)	109.1319		
H(4)	N(1)	1.0163	C(2)	107.3383	O(3)	101.0466
H(5)	C(2)	1.0964	N(1)	113.3050	O(3)	-51.0734
H(6)	C(2)	1.0896	N(1)	108.9588	H(5)	109.4320
H(7)	C(2)	1.0889	N(1)	107.8619	H(5)	109.0939
H(8)	O(3)	0.9655	N(1)	104.9839	C(2)	-15.0604

Table B.25. N-methylhydroxylamine d) structure optimized at the MP2/Aug-cc-pVTZ theory level.

Atom 1	Atom 2	Bond Length (Angstroms)	Atom 3	Angle (degrees)	Atom 4	Torsion Angle (degrees)
N(1)						
C(2)	N(1)	1.4570				
O(3)	N(1)	1.4587	C(2)	105.5573		
H(4)	N(1)	1.0167	C(2)	107.5265	O(3)	105.6011
H(5)	C(2)	1.0928	N(1)	113.3193	O(3)	-55.9024
H(6)	C(2)	1.0867	N(1)	108.3641	H(5)	109.0149
H(7)	C(2)	1.0897	N(1)	107.4380	H(5)	109.9228
H(8)	O(3)	0.9642	N(1)	105.9129	C(2)	122.2019

Appendix C

Triplet Structures

C.1 Triplet Methanediol

Table C.01. Methanediol structure optimized at the MP2/Aug-cc-pVTZ theory level.

Atom 1	Atom 2	Bond Length (Angstroms)	Atom 3	Angle (degrees)	Atom 4	Torsion Angle (degrees)
C(1)						
O(2)	C(1)	1.6698				
O(3)	C(1)	1.6698	O(2)	71.4376		
H(4)	C(1)	1.0695	O(2)	117.0582	O(3)	105.7301
H(5)	C(1)	1.0695	O(2)	105.7301	O(3)	117.0582
H(6)	O(2)	0.9717	C(1)	105.3511	O(3)	-79.6904
H(7)	O(3)	0.9717	C(1)	105.3511	O(2)	-79.6904

C.2 Triplet Aminomethanol

Table C.02. Aminomethanol a) structure optimized at the MP2/Aug-cc-pVTZ theory level.

Atom 1	Atom 2	Bond Length (Angstroms)	Atom 3	Angle (degrees)	Atom 4	Torsion Angle (degrees)
N(1)						
C(2)	N(1)	1.4471				
O(3)	C(2)	1.3853	N(1)	113.5390		
H(4)	N(1)	1.0474	C(2)	121.1155	O(3)	-5.8436
H(5)	N(1)	1.0733	C(2)	119.9091	H(4)	118.8473
H(6)	C(2)	1.0966	N(1)	105.4622	O(3)	114.6120
H(7)	C(2)	1.0922	N(1)	106.5173	O(3)	108.8575
H(8)	O(3)	0.9653	C(2)	109.2302	N(1)	76.3123

Table C.03. Aminomethanol b) structure optimized at the MP2/Aug-cc-pVTZ theory level.

Atom 1	Atom 2	Bond Length (Angstroms)	Atom 3	Angle (degrees)	Atom 4	Torsion Angle (degrees)
N(1)						
C(2)	N(1)	1.4245				
O(3)	C(2)	1.3943	N(1)	108.8180		
H(4)	N(1)	1.0376	C(2)	120.3367	O(3)	-0.0431
H(5)	N(1)	1.1011	C(2)	118.9276	H(4)	120.7358
H(6)	C(2)	1.0994	N(1)	105.9493	O(3)	114.1628
H(7)	C(2)	1.0994	N(1)	105.9530	O(3)	114.1613
H(8)	O(3)	0.9646	C(2)	108.8891	N(1)	179.8258

Table C.04. Aminomethanol c) structure optimized at the MP2/Aug-cc-pVTZ theory level.

Atom 1	Atom 2	Bond Length (Angstroms)	Atom 3	Angle (degrees)	Atom 4	Torsion Angle (degrees)
N(1)						
C(2)	N(1)	1.4268				
O(3)	C(2)	1.3945	N(1)	109.0939		
H(4)	N(1)	1.0383	C(2)	120.3879	O(3)	-1.0110
H(5)	N(1)	1.0967	C(2)	119.1358	H(4)	120.4726
H(6)	C(2)	1.0985	N(1)	105.9599	O(3)	114.2864
H(7)	C(2)	1.0988	N(1)	105.9069	O(3)	113.7535
H(8)	O(3)	0.9644	C(2)	108.8640	N(1)	158.6363

Bibliography

[1] Miller, S. L.; Cleaves, H. J. In *Systems Biology: Genomics*, Vol. 1, Rigoutsos, I; Stephanopoulos, G, Eds.; Oxford University Press: New York, 2007; 3-56.

[2] Snyder, L. E. The search for interstellar glycine. *Origins of Life and Evolution of the Biosphere* (1997), **27**, 115-133.

[3] Garrod, R. T.; Widicus Weaver, S. L.; Herbst, E. Complex chemistry in star-forming regions: an expanded gas-grain warm-up chemical model. *Astrophysical Journal* (2008), **682**, 283-302.

[4] Wilson, E. First Molecular Anion Identified In Space. *Chemical & Engineering News* (2006), 84(48), 5.

[5] McCall B. J.; Huneycutt A. J.; Saykally R. J.; Geballe T. R.; Djuric N.; Dunn G. H.; Semaniak J.; Novotny O.; Al-Khalili, A.; Ehlerding A.; Hellberg F.; Kalhori S.; Neau A.; Thomas R.; Osterdahl F.; Larsson M. An enhanced cosmic-ray flux towards ζ Persei inferred from a laboratory study of the $H3^+$-e^- recombination rate. *Nature* (2003), **422**(6931), 500-502.

[6] Perri, M. J.; Van Wyngarden, A. L.; Lin, J. J.; Lee, Y. T.; Boering, K. A.. Energy Dependence of Oxygen Isotope Exchange and Quenching in the $O(^1D) + CO_2$ Reaction: A Crossed Molecular Beam Study. *Journal of Physical Chemistry A* 2004, **108**, 7995-8001.

[7] Hermans, C.; Vandaele, A. C.; Carleer, M.; Fally, S.; Colin, R.; Jenouvrier, A.; Coquart, B.; Merienne, M. F.. Absorption cross - sections of atmospheric constituents. NO_2, O_2, and H_2O. *Environmental Science and Pollution Research International* (1999), **6**(3), 151-158.

[8] Lu, Y.; Liang, C.; Lin, J. J. Crossed molecular beam studies on the reaction dynamics of $O(^1D) + N_2O$. *Journal of Chemical Physics* (2006), **125**(13), 133121/1-133121/8.

[9] Balucani, N.; Casavecchia, P.; Aoiz, F. J.; Banares, L.; Castillo, J. F.; Herrero, V. J. Dynamics of the $O(^1D)+D_2$ reaction: A comparison between crossed molecular beam experiments and quasiclassical trajectory calculations on the lowest three potential energy surfaces. *Molecular Physics* (2005), **103**(13), 1703-1714.

[10] Aoiz, F. J.; Banares, L.; Castillo, J. F.; Herrero, V. J.; Martinez-Haya, B. A quasiclassical trajectory and quantum mechanical study of the $O(^1D) + D_2$ reaction dynamics. Comparison with high resolution molecular beam experiments. *Physical Chemistry Chemical Physics* (2002), **4**(18), 4379-4385.

[11] Shu, J.; Lin, J. J.; Lee, Y. T.; Yang, X. Multiple pathway dynamics of the $O(1D)+C_2H_6$ reaction: A crossed beam study. *Journal of Chemical Physics* (2001), **115**(2), 849-857.

[12] Shu, J.; Lin, J. J.; Wang, C. C; Lee, Y. T.; Yang, X. Crossed molecular beam studies of the $O(1D)+NH_3$ reaction. *Journal of Chemical Physics* (2001), **115**(2), 842-848.

[13] Buss, R. J.; Casavecchia, P.; Hirooka, T.; Sibener, S. J.; Lee, Y. T. Reactive scattering of atomic oxygen(1D) + diatomic hydrogen. *Chemical Physics Letters* (1981), **82**(3), 386-91.

[14] Ralchenko, Y.; Kramida, A. E.; Reader, J.; NIST ASD Team. *NIST Atomic Spectra Database* (2008) (version 3.1.5), , National Institute of Standards and Technology, Gaithersburg, MD. http://physics.nist.gov/asd3 [2010, February 23].

[15] Wiese, W. L.; Fuhr, J. R.; Deters, T. M. *Atomic transition probabilities of carbon, nitrogen, and oxygen. A critical data compilation. Journal of Physical and Chemical Reference Data, Monograph* (1996), **7**, 552.

[16] Carl, S. A. A highly sensitive method for time-resolved detection of $O(^1D)$ applied to precise determination of absolute $O(^1D)$ reaction rate constants and $O(^3P)$ yields. *Physical Chemistry Chemical Physics* (**2005)**, **7**, 4051-4053.

[17] Yang, X. Multiple channel dynamics in the O(1D) reaction with alkanes. *Physical Chemistry Chemical Physics* (2006), **8**(2), 205-215.

[18] Kurosaki, Y.; Takayanagi, T. Ab initio molecular orbital study of the $O(^1D)$ insertion into the C-C bond in cyclopropane and ethane. *Chemical Physics Letters* (2002), **355**(5,6), 424-430.

[19] Vranckx, S.; Peeters, J.; Carl, S. A temperature dependence kinetic study of $O(^1D)$ + CH_4: overall rate coefficient and product yields. *Physical Chemistry Chemical Physics* (2008), **10**(37), 5714-5722.

[20] Lugez, C.; Schriver, A.; Levant, R.; Schriver-Mazzuoli, L. A matrix-isolation infrared spectroscopic study of the reactions of methane and methanol with ozone. *Chemical Physics* (1994), **181**, 129-46.

[21] Lu, I. C.; Lin, J. J.; Lee, S. H.; Lee, Y. T.; Yang, X. Product angular anisotropy in CO_2 photodissociation at 157 nm. *Chemical Physics Letters* (2003**)**, **382**, 665-670.

[22] Nishida, S.; Taketani, F.; Takahashi, K.; Matsumi, Y. Quantum Yield for $O(^1D)$ Production from Ozone Photolysis in the Wavelength Range of 193-225 nm. *Journal of Physical Chemistry A* (2004), **108**, 2710-2714.

[23] Shafer, N.; Tonokura, K.; Matsumi, Y.; Tasaki, S.; Kawasaki, M. The Doppler spectra of $O(^1D)$ from the photodissociation of O_2, NO_2, and N_2O. *Journal of Chemical Physics (*1991), **95**, 6218-6223.

[24] Lambert, H. M.; Dixit, A. A.; Davis, E. W.; Houston, P. L. Quantum yields for product formation in the 120-133 nm photodissociation of O_2. *Journal of Chemical Physics* (2004**)**, **121**, 10437-10446.

[25] Atkinson, R.; Baulch, D. L.; Cox, R. A.; Hampson, R. F. Jr.; Kerr, J. A.; Rossi, M. J.; Troe, J. IUPAC Subcommittee on Gas Kinetic Data Evaluation for Atmospheric Chemistry. *Journal of Physical and Chemical Reference Data* [Online] (1997**)**, **26**, 1329

[26] Schinke, R.; Grebenshchikov, S. Y.; Zhu, H. The photodissociation of NO_2 in the second absorption band: Ab initio and quantum dynamics calculations. *Chemical Physics* (2008), **346**, 99-114.

[27] Pauli, W. The Connection between Spin and Statistics. Physical Review (1940), **58**(8), 716 -722.

[28] Pauli, W.. Relativistic Field Theories of Elementary Particles. *Reviews of Modern Physics* (1941), **13**(3), 203-232.

[29] Moore, G.; Seiberg, N. Classical and Quantum Conformal Field Theory. *Communications in Mathematical Physics* (1989), **122**, 177-254.

[30] Zhu, Y. F.; Gordon, R. J. The production of $O(^3P)$ in the 157 nm photodissociation of CO_2. *Journal of Chemical Physics* (1990), **92**, 2897-2901.

[31] Sun, J.; Tang, Y.; Jia, X.; Wang, F.; Sun, H.; Feng, J.; Pan, X.; Hao, L.; Wang, R. Theoretical study for the reaction of CH_3CN with $O(^3P)$. *Journal of Chemical Physics* (2010), **132**(6), 064301/1-064301/13.

[32] Vranckx, S.; Peeters, J.; Carl, S. A. Absolute rate constant and $O(^3P)$ yield for the $O(^1D)+N_2O$ reaction in the temperature range 227 K to 719 K. *Atmospheric Chemistry and Physics* (2008), **8**(20), 6261-6272.

[33] Casavecchia, P.; Capozza, G.; Segoloni, E.; Leonori, F.; Balucani, N.; Volpi, G. G. Dynamics of the $O(^3P) + C_2H_4$ Reaction: Identification of Five Primary Product Channels (Vinoxy, Acetyl, Methyl, Methylene, and Ketene) and Branching Ratios by the Crossed Molecular Beam Technique with Soft Electron Ionization. *Journal of Physical Chemistry A* (2005), **109**(16), 3527-3530.

[34] Avallone, L. M. Measurements of the temperature-dependent rate coefficient for the reaction $O(^3P) + NO_2 \rightarrow NO + O_2$. *Journal of Photochemistry and Photobiology, A: Chemistry* (2003), **157**(2-3), 231-236.

[35] Leonori, F.; Balucani, N.; Capozza, G.; Segoloni, E.; Stranges, D.; Casavecchia, P. Crossed beam studies of radical-radical reactions: $O(^3P) + C_3H_5$ (allyl). *Physical Chemistry Chemical Physics* (2007), **9**(11), 1307-1311.

[36] Choi, J. H. Radical-radical reaction dynamics: a combined crossed-beam and theoretical study. *International Reviews in Physical Chemistry* (2006), **25**(4), 613-653.

[37] Conforti, P. F.; Braunstein, M.; Dodd, J. A. Energetics and Dynamics of the Reactions of $O(^3P)$ with Dimethyl Methylphosphonate and Sarin. *Journal of Physical Chemistry A* (2009), **113**(49), 13752-13761.

[38] Ballinger, P.; Long, F. A. Acid ionization constants of alcohols. II. Acidities of some substituted methanols and related compounds. *Journal of the American Chemical Society* (1960), **82** 795-8.

[39] Funderburk, L. H.; Aldwin, L.; Jencks, W. P. Mechanisms of general acid and base catalysis of the reactions of water and alcohols with formaldehyde. *Journal of the American Chemical Society* (1978), **100**(17), 5444-59.

[40] Spangler, D.; Williams, I. H.; Maggiora, G. M. Determination and characterization of a transition structure for water-formaldehyde addition. *Journal of Computational Chemistry* (1983), **4**(4), 524-41.

[41] Le Botlan, D. J.; Mechin, B. G.; Martin, G. J. Proton and carbon-13 nuclear magnetic resonance spectrometry of formaldehyde in water. *Analytical Chemistry* (1983), **55**(3), 587-91.

[42] Utterback, D. F.; Millington, D. S.; Gold, A. Characterization and determination of formaldehyde oligomers by capillary column gas chromatography. *Analytical Chemistry* (1984), **56**(3), 470-473.

[43] Gold, A.; Utterback, D. F.; Millington, D. S. Quantitative analysis of gas-phase formaldehyde molecular species at equilibrium with formalin solution. *Analytical Chemistry* (1984), **56**(14), 2879-2882.

[44] Mohlmann, G. R. Raman spectra of aqueous solutions of formaldehyde and its oligomers. *Journal of Raman Spectroscopy* (1987), **18**(3), 199-203.

[45] Brandani, S.; Brandani, V.; Tarquini, I. Vapor-Liquid Equilibrium of Formaldehyde Mixtures Containing Methanol. *Industrial & Engineering Chemistry Research* (1998), **37**(8), 3485-3489.

[46] Winkelman, J. G. M.; Voorwinde, O. K.; Ottens, M.; Beenackers, A. A. C. M.; Janssen, L. P. B. M. Kinetics and chemical equilibrium of the hydration of formaldehyde. *Chemical Engineering Science* (2002), **57**(19), 4067-4076.

[47] Kent, D. R. IV; Widicus, S. L.; Blake, G. A.; Goddard, W. A. III. A theoretical study of the conversion of gas phase methanediol to formaldehyde. *Journal of Chemical Physics* (2003), **119**(10), 5117-5120.

[48] Maiwald, M.; Fischer, H. H.; Ott, M.; Peschla, R.; Kuhnert, C.; Kreiter, C. G.; Maurer, G.; Hasse, H. Quantitative NMR Spectroscopy of Complex Liquid Mixtures: Methods and Results for Chemical Equilibria in Formaldehyde-Water-Methanol at Temperatures up to 383 K. *Industrial & Engineering Chemistry Research* (2003), **42**(2), 259-266.

[49] Ottosson, N.; Aziz, E. F.; Bradeanu, I. L.; Legendre, S.; Oehrwall, G.; Svensson, S.; Bjoerneholm, O.; Eberhardt, W. An electronic signature of hydrolysation in the X-ray absorption spectrum of aqueous formaldehyde. *Chemical Physics Letters* (2008), **460**(4-6), 540-542.

[50] Ottosson, N.; Aziz, E. F.; Bergersen, H.; Pokapanich, W.; Ohrwall, G.; Svensson, S.; Eberhardt, W.; Bjorneholm, O. Electronic Rearrangement upon the Hydrolyzation of Aqueous Formaldehyde Studied by Core-Electron Spectroscopies. *Journal of Physical Chemistry B* (2008), **112**(51), 16642-16646.

[51] Ervens, B.; Herckes, P.; Feingold, G.; Lee, T.; Collett, J. L. Jr.; Kreidenweis, S. M. On the Drop-Size Dependence of Organic Acid and Formaldehyde Concentrations in Fog. *Journal of Atmospheric Chemistry* (2003), **46**(3), 239-269.

[52] Zhao, X.; Turco, R. P. Photodissociation parameterization for stratospheric photochemical modeling. *Journal of Geophysical Research, [Atmospheres]* (1997), **102**(D8), 9447-9459.

[53] Pandis, S. N.; Seinfeld, J. H. Sensitivity analysis of a chemical mechanism for aqueous-phase atmospheric chemistry. *Journal of Geophysical Research, [Atmospheres]* (1989), **94**(D1), 1105-26.

[54] Chenier, P. J.; Ed. *Survey of Industrial Chemistry*, 3rd ed.; Kluwer Academic / Plenum Publishers: New York (2002).

[55] Hosaus, H.; Rave, P.; Wigand, P.; Tollens, B. The synthesis of polyhydric alcohols by means of formaldehyde. *Journal of the American Chemical Society* (1893), **15**(12), 704-8.

[56] Oro, J.; Kimball, A.; Fritz, R.; Master, F.. Amino acid synthesis from formaldehyde and hydroxylamine. *Archives of Biochemistry and Biophysics* (1959), **85** 115-30

[57] Fox, S. W.; Windsor, C. R. Synthesis of amino acids by the heating of formaldehyde and ammonia. *Science* (1970), **170**(3961), 984-6

[58] Hulett, H. R.; Wolman, Y.; Miller, S. L.; Ibanez, J.; Oró, J.; Fox, S. W.; Windsor, C. R. Formaldehyde and ammonia as precursors to prebiotic amino acids. *Science* (1971), **174**(13), 1038-41.

[59] Snyder, L. E.; Buhl, D.; Zuckerman, B.; Palmer, P. Microwave detection of interstellar formaldehyde. *Physical Review Letters* (1969), **22**(13), 679-81.

[60] Wakai, C.; Morooka, S.; Matubayasi, N.; Nakahara, M. Carbon-carbon bond formation in glycolic acid generated spontaneously from dichloromethane in hot water. *Chemistry Letters* (2004), **33**(3), 302-303.

[61] Johnson, R. A.; Stanley, A. E. GC/MS and FT-IR spectra of methoxymethanol. *Applied Spectroscopy* (1991), 45(2), 218-22.

[62] Zabidi, N. A. M.; Tapp, D.; Thomas, T. F. Kinetics of the Rapid Dark Reaction between Methanol and Oxygen in the Presence of a "Photocatalyst". *Journal of Physical Chemistry* (1995), 99(40), 14733-7.

[63] Lugez, C.; Schriver, A.; Levant, R.; Schriver-Mazzuoli, L. A matrix-isolation infrared spectroscopic study of the reactions of methane and methanol with ozone. *Chemical Physics* (1994), 181(1-2), 129-46.

[64] Wrobel, R.; Sander, W.; Kraka, E.; Cremer, D. Reactions of dimethyl ether with atomic oxygen : a matrix isolation and a quantum chemical study. *Journal of Physical Chemistry A* (1999), **103**(19), 3693-3705.

[65] Ogata, Y.; Kawasaki, A. Kinetics of the reaction of formaldehyde with ammonia. Bulletin of the Chemical Society of Japan (1964), **37**(4), 514-19.

[66] Minyaev, R. M.; Lepin, E. A. Gradient line reaction path of ammonia addition to formaldehyde. *Mendeleev Communications* (1997), **5**, 189-191.

[67] Bossa, J. B.; Theule, P.; Duvernay, F.; Chiavassa, T. NH_2CH_2OH thermal formation in interstellar ices contribution to the 5-8 μm region toward embedded protostars. *Astrophysical Journal* (2009), **707**, 1524-1532.

[68] Møller, C.; Plesset, M. S. Note on an Approximation Treatment for Many-Electron Systems. *Physical Review* (1934), **46**, 618–622.

[69] Head-Gordon, M.; Pople, J. A.; Frisch, M. J. MP2 Energy Evaluation by Direct Methods. *Chemical Physics Letters* (1988), **153**(6), 503-506.

[70] Dunning, T. H. Gaussian Basis Sets For Use in Correlated Molecular Calculations. I. The Atoms Boron Through Neon and Hydrogen. *Journal of Chemical Physics* (1989), **90**(2), 1007-1023.

[71] Dunning, T. H. A Road Map for the Calculation of Molecular Binding Energies. *Journal of Physical Chemistry A* (2000), **104**, 9062-9080.

[72] Gaussian 09, Revision A.02, M. J. Frisch, G. W. Trucks, H. B. Schlegel, G. E. Scuseria, M. A. Robb, J. R. Cheeseman, G. Scalmani, V. Barone, B. Mennucci, G. A. Petersson, H. Nakatsuji, M. Caricato, X. Li, H. P. Hratchian, A. F. Izmaylov, J. Bloino, G. Zheng, J. L. Sonnenberg, M. Hada, M. Ehara, K. Toyota, R. Fukuda, J. Hasegawa, M. Ishida, T. Nakajima, Y. Honda, O. Kitao, H. Nakai, T. Vreven, J. A. Montgomery, Jr., J. E. Peralta, F. Ogliaro, M. Bearpark, J. J. Heyd, E. Brothers, K. N. Kudin, V. N. Staroverov, R. Kobayashi, J. Normand, K. Raghavachari, A. Rendell, J. C. Burant, S. S. Iyengar, J. Tomasi, M. Cossi, N. Rega, J. M. Millam, M. Klene, J. E. Knox, J. B. Cross, V. Bakken, C. Adamo, J. Jaramillo, R. Gomperts, R. E. Stratmann, O. Yazyev, A. J. Austin, R. Cammi, C. Pomelli, J. W. Ochterski, R. L. Martin, K. Morokuma, V. G. Zakrzewski, G. A. Voth, P. Salvador, J. J. Dannenberg, S. Dapprich, A. D. Daniels, O. Farkas, J. B. Foresman, J. V. Ortiz, J. Cioslowski, and D. J. Fox, Gaussian, Inc., Wallingford CT, 2009.

[73] Brooks, B. R.; Bruccoleri, R. E.; Olafson, B. D.; States, D. J.; Swaminathan, S.; Karplus, M. CHARMM: a program for macromolecular energy, minimization, and dynamics calculations. *Journal of Computational Chemistry* (1983), **4**(2), 187-217.

[74] ACD/ChemSketch Freeware, version 10.00, Advanced Chemistry Development, Inc., Toronto, ON, Canada, www.acdlabs.com, 2006.

[75] Anderson, T.; Herbst, E.; DeLucia, F. C. An extension of the high-resolution millimeter- and submillimeter-wave spectrum of methanol to high angular momentum quantum numbers. *The Astrophysical Journal Supplement Series* (1992), **82,** 405–444.

[76] Lovus, F. J.; Lutz, H.; Dreizler, H. Microwave-Spectra of Molecules of Astrophysical Interest .XVII. Dimethyl Ether. *Journal of Physical and Chemical Reference Data* (1979), **8**, 1051 -1107.

[77] Ilyushina,V. V.; Alekseeva, E. A.; Dyubkoa, S. F.; Motiyenkoa, R. A.; Hougen, J. T. The Rotational Spectrum of the Ground State of Methylamine. *Journal of Molecular Spectroscopy* (2005), **229**, 170–187.

[78] Peng, C.; Schlegel, H. B. Combining Synchronous Transit and Quasi-Newton Methods to Find Transition States. *Israel Journal of Chemistry* (1993), **33**, 449-454.

[79] Kent, D. R. IV; Widicus, S. L.; Blake, G. A.; Goddard, W. A. III. A theoretical study of the conversion of gas phase methanediol to formaldehyde. *Journal of Chemical Physics* (2003), **119**(10), 5117-5120.

[80] Hu, S.; Wang, X.; Chu, T.; Liu, X. Influence of H_2 on the Gas-Phase Decomposition of Formic Acid: *A Theoretical Study*. *Journal of Physical Chemistry A* (2005), **109**(40), 9129-9140.

[81] Wrobel, R.; Sander, W.; Kraka, E.; Cremer, D. Reactions of dimethyl ether with atomic oxygen : a matrix isolation and a quantum chemical study. *Journal of Physical Chemistry A* (1999), **103**(19), 3693-3705.

[82] Feldmann, M. T.; Widicus, S. L.; Blake, G. A.; Kent, D. R. IV; Goddard, W. A. III. Aminomethanol water elimination: Theoretical examination. *Journal of Chemical Physics* (2005), **123**(3), 034304/1-034304/6.

[83] Sung, E.; Harmony, M. D. Microwave spectrum, structure, quadrupole coupling constants, dipole moment, and barrier to internal rotation of N-methylhydroxylamine. *Journal of Molecular Spectroscopy* (1979), **74**(2), 228-41.

[84] Pickett, H. M. The fitting and prediction of vibration-rotation spectra with spin interactions. *Journal of Molecular Spectroscopy* (1991), **148**(2), 371-7.

[85] Yu, S.; Drouin, B. J. Terahertz spectroscopy of the ground state of methylamine (CH_3NH_2). *64th Ohio State University International Symposium on Molecular Spectroscopy*, HW11, 2009.